Hydration-Coupled Dynamics in Proteins Studied by Neutron Scattering and NMR: The Case of the Typical EF-Hand Calcium-Binding Parvalbumin

Jean-Marc Zanotti,* Marie-Claire Bellissent-Funel,* and Joseph Parello#

*Laboratoire Léon Brillouin (CEA-CNRS), CEA-Saclay, 91191 Gif-sur-Yvette Cedex, France; and #UPRES-A 5074 CNRS, Faculté de Pharmacie, 34060 Montpellier Cedex 2, France and Burnham Institute, La Jolla, California 92037 USA

ABSTRACT The influence of hydration on the internal dynamics of a typical EF-hand calciprotein, parvalbumin, was investigated by incoherent quasi-elastic neutron scattering (IQNS) and solid-state ^{13}C-NMR spectroscopy using the powdered protein at different hydration levels. Both approaches establish an increase in protein dynamics upon progressive hydration above a threshold that only corresponds to partial coverage of the protein surface by the water molecules. Selective motions are apparent by NMR in the 10-ns time scale at the level of the polar lysyl side chains (externally located), as well as of more internally located side chains (from Ala and Ile), whereas IQNS monitors diffusive motions of hydrogen atoms in the protein at time scales up to 20 ps. Hydration-induced dynamics at the level of the abundant lysyl residues mainly involve the ammonium extremity of the side chain, as shown by NMR. The combined results suggest that peripheral water-protein interactions influence the protein dynamics in a global manner. There is a progressive induction of mobility at increasing hydration from the periphery toward the protein interior. This study gives a microscopic view of the structural and dynamic events following the hydration of a globular protein.

INTRODUCTION

It is widely accepted that dynamics and function are intimately correlated in biological macromolecules (Nienhaus et al., 1997). Although a large body of experimental and theoretical evidence substantiates this view, there are still challenges which are far from being reached in this respect. As emphasized by Frauenfelder (1995a,b) complexity in proteins leaves most of these challenges only with partial answers. It has also been recognized through the pioneering work of Careri and Rupley (for a review see Rupley and Careri, 1991) that hydration plays a crucial role in this correlation (see also Frauenfelder and Gratton, 1986). Protein hydration has been a central theme in structural biology for more than 50 years (Perutz, 1946; for a review see Westhof, 1993). As shown by x-ray and neutron crystallography, water is highly organized at the interface between the protein and bulk water (Thanki et al., 1988; Frey, 1993; Savage and Wlodawer, 1986). Such studies substantiate the view that structurally defined water sites are part of the protein tertiary fold. However, besides information on the amplitudes of internal motions, as inferred from atomic temperature factors, such crystallographic studies provide no information on the time scales associated with protein dynamics, as well as with the dynamics of the hydration water molecules themselves. The dynamics of the latter at the protein surface have recently been investigated in a selective manner by inelastic neutron scattering spectroscopy using H_2O-hydrated powders of a totally deuterated protein (Bellissent-Funel et al., 1993; 1996). Finally, in the case of proteins in solution, structurally defined water sites have been characterized through the dynamical and kinetic properties of the corresponding water molecules using correlated multidimensional NMR spectroscopy (Otting et al., 1991; Qian et al., 1993; Wider et al., 1998). Nuclear magnetic relaxation dispersion of the magnetic water isotopes ^1H, ^2H, and ^{17}O is also a major source of information about hydration of biomolecules giving access to a detailed description of the dynamical properties of specific water molecules in proteins (Bryant, 1996).

The characteristic times of motions in proteins at physiological temperatures range over more than 12 orders of magnitude, from below picoseconds to well above seconds (Frauenfelder, 1989; McCammon, 1984). Since proteins are densely packed (Richards, 1977) and their compressibility is low in comparison to liquids and solid polymers (Gavish et al., 1983) conformational variations can only occur in a concerted manner, with the consequence that motions in the fast dynamics regime (picosecond time scale) with relatively small atomic displacements may act as precursors of much slower motions of functional relevance, with larger amplitudes, in a hierarchical manner as initially proposed by Frauenfelder and co-workers (Ansari et al., 1985). Large-amplitude motions in the protein interior, in the millisecond time scale, are the flipping motions about the C_β-C_1 bonds of the phenylalanine and tyrosine aromatic rings (for a review see Gurd and Rothgeb, 1979). An example of such a hierarchy could involve hinge and/or shear motions between domains that have been inferred from x-ray crystallography with a variety of proteins for which open and closed conformational states are available (Gerstein et al., 1994).

A rather unique tool used to gain experimental information on protein dynamics in the picosecond range (from 0.1 to a few hundred picoseconds) is incoherent inelastic neu-

Received for publication 31 July 1998 and in final form 13 January 1999.

Address reprint requests to Dr. Marie-Claire Bellissent-Funel, Laboratoire Léon Brillouin (CEA-CNRS), CEA-Saclay, 91191 Gif-sur-Yvette Cedex, France. Tel.: 33 1 6908 6066; Fax: 33 1 6908 82 61; E-mail: mcbel@llb.saclay.cea.fr.

0006-3495/99/05/2390/22 $2.00

tron scattering (IINS), which takes advantage of the large incoherent scattering cross-section of hydrogen atoms with respect to the relatively small cross-sections of other constitutive atoms in proteins. In such experiments, the scattered intensity is observed as a function of the transfer momentum $\hbar Q$ and of the energy, $\hbar\omega$, transferred to the protein. A large fraction of the atoms (up to 50%) in globular proteins are hydrogen atoms, and since they are distributed nearly homogeneously within the protein molecule, IINS will thus allow protein dynamics to be characterized in a global manner by monitoring the dynamics of hydrogen atoms. However, as recently emphasized by Frauenfelder (1998), "to get deeper insight into function, global data are not enough; the information must be specific." Selective substitution of hydrogen atoms by deuterium atoms can be used in principle to monitor the dynamics of hydrogen subpopulations by IINS since the incoherent scattering cross-section of deuterium atoms is 40 times smaller than that of hydrogen atoms (Lovesey, 1987). This is readily achieved in the case of exchangeable hydrogen atoms, but selective substitution of nonexchangeable hydrogen atoms from one (or several) class(es) of amino acid residues can also be achieved through biosynthetic approaches (Réat et al., 1998 and references therein). IINS has been used to investigate the internal dynamics of a variety of biological macromolecules and macromolecular assemblies. In a pioneering study of hexokinase in solution, Jacrot et al. (1982) compared the dynamics of the enzyme in the presence and in the absence of bound glucose and showed that the enzyme with its substrate bound to the catalytic cleft is more dynamically constrained than the enzyme in the absence of glucose. Subsequently, IINS studies of protein dynamics have been performed with hydrated protein powders. In contrast to protein solutions, powders allow controlled variations of water activity to be achieved over a wide range from a dehydrated state (usually including a restricted number of constitutive water molecules) to hydrated states of the protein resulting in partial or "monolayer" coverage of the protein surface by water molecules. Protein powders hydrated with heavy water (D_2O) offer the advantage of limiting the incoherent contribution from the solvent to the total scattered intensity. Several globular proteins have been studied so far by IINS as D_2O-hydrated powders, including myoglobin (Doster et al., 1989; Cusack and Doster, 1990) and superoxide dismutase (Andreani et al., 1995). In such studies, special attention was focused on the influence of temperature on protein dynamics by monitoring the temperature-dependent intensity variations of the elastic component in the IINS spectrum. This led to the discovery of a glassy transition in myoglobin in the 180 K temperature range (Doster et al., 1989). Above this critical temperature protein motions become anharmonic instead of the harmonic regime observed below this temperature. This transition is apparently common to other hydrated globular proteins investigated so far by IINS (Ferrand et al., 1993; Réat et al., 1997; Fitter et al., 1997). Such experimental observations provide strong evidence that hydration plays an essential role in protein dynamics. The observation that hydrated lysozyme powders, at relatively low hydration (>0.2 g water/g dry protein), display enzymatic activity suggests that there is a correlation between hydration, dynamics, and function in proteins (Rupley and Careri, 1991). A similar conclusion has been recently achieved in the case of bacteriorhodopsin within the purple membrane (Réat et al., 1998).

As far as proteins in the solid state (powdered and crystalline materials) are concerned, a parallel approach for investigating internal dynamics in proteins in a site-specific manner is given by magic angle spinning (MAS) solid-state ^{13}C-NMR. MAS averages the second-rank chemical shift tensor by rotating the sample about an axis inclined at a 54° 44′ angle with respect to the external magnetic field so that the spectrum is composed of peaks at the isotropic shifts of each resonance (comparable, if not identical, to the chemical shifts inferred from solution ^{13}C-NMR spectra). This technique provides high-resolution NMR spectra of solids with lineshapes comparable to those in solution, although residual broadening is the rule in proteins. In the absence of rotational diffusion, in contrast to liquids, solid-state natural-abundance ^{13}C-NMR of powdered or crystalline polymers affords information on internal dynamics in a direct manner (Komoroski, 1986). Studies of protein dynamics in the solid state have thus benefited from the availability and advances of solid-state NMR spectroscopy (Opella, 1997). More specifically, the influence of hydration on protein dynamics in the solid state has been investigated by MAS ^{13}C-NMR spectroscopy in the case of powdered lysozyme (Kennedy and Bryant, 1990; Gregory et al., 1993a) and bovine serum albumin (Gregory et al., 1993b).

With the goal of understanding the role of internal dynamics on protein function in calciproteins, we decided to investigate the role of hydration on the internal dynamics of parvalbumin (Pa), a representative of the large family of evolutionary related proteins, the so-called EF-hand proteins, including troponin C, calmodulin, and parvalbumin, as well as a variety of other subfamilies (Kawasaki and Kretsinger, 1994). All EF-hand proteins have in common the possibility of binding Ca^{2+} as well as Mg^{2+}, two cations that appear to be of the highest physiological relevance in cell excitation and relaxation. Due to their high affinities for Ca^{2+} (k_{Ca} in the 10^{-9} M range for parvalbumin; Cavé et al., 1979b), the EF-hand proteins will primarily sense intracellular Ca^{2+} concentration variations upon cell excitation and relaxation, whereas the intracellularly abundant Mg^{2+} ions (mM range), although competing with affinities by several orders of magnitude less, will be replacing Ca^{2+} upon variation of the intracellular Ca^{2+} concentration. In this physiological context, parvalbumin appears as an efficient relaxing factor in a variety of Ca^{2+}-excitable cells in vertebrates, as in muscle cells and in specific neurons (Celio, 1986; Rüegg, 1989; Hartig et al., 1996).

Our choice of parvalbumin was guided by the fact that this typical EF-hand protein has been recognized for more than 25 years as a single domain globular protein with

characteristic dynamical properties at the level of its internal hydrophobic domain (Parello and Pechère, 1971; Opella et al., 1974; Cavé et al., 1976; Nelson et al., 1976; Cavé and Parello, 1981). Internal rotation of the Phe aromatic rings (flipping motions around the C_β-C_1 bonds) occurs at a rate faster than 10^3 s^{-1} at ambient temperature as inferred from ^{1}H-NMR lineshape evidence (Cavé et al., 1976). Interestingly, such slow dynamics, in the microsecond-millisecond time scale, are basically conserved during evolution likely due to the high invariance of the residues that make up the hydrophobic core of parvalbumin (Cavé and Parello, 1981). Using the Woessner model for predicting internal anisotropic reorientation times (τ_i), Nelson et al. (1976) found that the C_α-C_β axis of the Phe residues also contributes to the internal dynamics with $\tau_i = \sim 4$ ns (to be compared with an overall isotropic reorientation time of 12 ns). These combined studies of parvalbumin by ^{1}H-NMR spectroscopy (lineshape analysis) and one-dimensional ^{13}C-NMR spectroscopy (relaxation parameters) unambiguously indicated in the mid-1970s that the hydrophobic core of parvalbumin displays an extended repertoire of dynamical events that are likely to involve most of the side chains within the protein core, besides the abundant Phe residues. The finding by Bauer et al. (1974) that the ^{13}C relaxation parameters for the α carbons of parvalbumin are the same as could be calculated from the overall tumbling time (determined independently by depolarized light scattering) implies that these carbons are an integral part of a rigid body and their motion is nearly isotropic. Recently, through measurements of ^{13}C-relaxation rates and heteronuclear NOEs of parvalbumin α carbons at natural abundance by two-dimensional spectroscopy, as well as by using a model-free approach for treating the relaxation data, Alattia et al. (1996) have reported a site-by-site description of the dynamics of nearly all ^{1}H-^{13}C vectors associated with the α carbons of the protein, with effective internal correlation times in the 1–65 ps range. In contrast to the aforementioned results by Nelson et al. (1976), no slow internal motions with characteristic times in the nanosecond range were reported by Alattia et al. (1996). It might be that both types of motion coexist in parvalbumin, as recently emphasized by Korzhnev et al. (1997) in their caveat about the applicability of the mode-free approach. The recent identification by x-ray crystallography at low temperature (100 K) with crystals diffracting at 0.91 Å resolution (Declercq et al., 1999; submitted for publication) of several conformational substates of parvalbumin with positional variations in the angstrom range (involving internal side chains of Phe, Val, and Ile, as well as the main chain), indicates that parvalbumin needs to be considered as a highly integrated dynamical assembly with localized and general motions. Are all these motions converging toward parvalbumin function? As established by x-ray crystallography (Declercq et al., 1991), both Ca^{2+}- and Mg^{2+}-loaded forms of parvalbumin differ by their conformations, although in a subtle manner in the sense that besides a slight rearrangement of their whole atomic packing a restricted number of conformational events (energy barrier-dependent) occur between the two forms. The analysis of the internal dynamics of both forms of parvalbumin is therefore of paramount importance. A study of the exchange rates of the amide NH groups in both forms by two-dimensional ^{1}H-NMR in solution has shown that both states of the protein, Ca^{2+}- and Mg^{2+}-loaded, respectively, differ by their exchange rates, thus suggesting differences in conformation and/or dynamics between the two states (Baldellon et al., 1992). Recently, a theoretical study combining molecular dynamics (in the picosecond range) and free-energy calculations (thermodynamic cycle) has given insight on the structural and dynamical features that characterize both forms of parvalbumin, Ca^{2+}- and Mg^{2+}-loaded (Allouche et al., 1999). Finally, hydration of parvalbumin has been characterized in detail by x-ray crystallography at high resolution, establishing the occurrence of a large variety of structurally well-defined water sites at the protein surface (Roquet et al., 1992). Among these water sites, 10 appear to be invariant during evolution. So far there is no experimental evidence to assess to which extent parvalbumin hydration is coupled to the internal dynamics of the protein.

We have addressed this question in this work through a combined analysis of the hydration-dependent dynamics of this typical EF-hand protein by IINS and natural-abundance MAS ^{13}C-NMR using powdered parvalbumin at controlled levels of hydration. The neutron scattering studies are focused on the quasi-elastic region of the IINS spectrum to probe diffusive motions in the 1–20 ps range, whereas NMR is sensitive to dynamical events, at specific sites of the tertiary structure (owing to the intrinsic resolution of the method), on a time scale of tens of ns. The dynamics of several subclasses of amino acid residues in parvalbumin, as well as their roles on the overall protein dynamics, are inferred from both experimental approaches, thus providing a first insight on hydration-coupled dynamics of this typical EF-hand protein. An account of this experimental approach has been recently reported (Zanotti et al., 1997).

MATERIALS AND METHODS

Samples

After separation of the two parvalbumin components from pike muscle (a minor component with pI 4.10 and a major component with pI 5.0) following a standard procedure (Pechère et al., 1971), the major component used in this work was desalted by dialysis against deionized and distilled water (Ca^{2+} content in the $2 \cdot 10^{-6}$ M range; pH = 5.7–5.8). Before lyophilization the protein was extensively dialyzed against de-ionized and distilled water. The dialysis step was followed by gel filtration using a column of Sephadex G50 (Pharmacia, Uppsala, Sweden) with sufficient capacity to retain residual salts. Under these conditions, the fractions following protein elution gave conductivities practically identical to that observed with water until residual salts retained on the column in the slowly eluting fractions gave rise to an increase in conductivity. Flame spectrophotometry measurements with the purified parvalbumin samples regularly gave a content of 2.0 Ca^{2+} ions/protein, corresponding to $PaCa_2$. The lyophilized protein was dried at constant weight in vacuo (10^{-6} Torr). Such a sample, which defines the "dry" protein ($h = 0$; see Fig. 3 and Fig. 6 *A*), still contains an extra quantity of matter that is eliminated at high temperature (150°C) corresponding to ~4% of the dry protein. This loss is

equated with residual water molecules, in agreement with crystallographic data (Roquet et al., 1992). Hydration was carried out by water diffusion in the vapor phase. $PaCa_2HHd$ corresponds to the normally protonated protein with all its hydrogen atoms, nonexchangeable and exchangeable in this order, present in the molecule, whereas the hydration water (indicated by *d*) exclusively involves deuterium atoms from D_2O. The protein with all its mobile hydrogen atoms preexchanged for deuterium (repeated lyophilization) and hydrated with D_2O is labeled $PaCa_2HDd$. Hydration with H_2O is indicated by *h*. Hydration is given by the symbol *h* in the text and expressed in g water/g dry protein.

Small angle neutron scattering (SANS) measurements and data analysis

The wavelength of the monochromatic neutron incident beam, λ, and the scattering angle θ define through the relation expressing momentum conservation during an elastic interaction, a scattering vector **Q**, with magnitude $Q = 4\pi \sin(\theta/2)/\lambda$. As in other scattering experiments, the scattered intensity is related to the structure of the sample, but in SANS experiments, the conditions are chosen in such a way that Q^{-1} is larger than the interatomic distances. The detailed description of the structure at the atomic level is therefore not possible, but this technique allows one to define the structural organization of the sample in the 10–500 Å range (Teixeira, 1992). SANS measurements were carried out on the PAXE spectrometer of the Reactor Orphée at the Laboratoire Léon Brillouin (LLB, Saclay, France), using an incident wavelength of 5 Å with the detector placed at 1.58 m, thus corresponding to a *Q* range of 0.023–0.4340 $Å^{-1}$. The intensity scattered by an assembly of identical centrosymmetric objects of density with coherent scattering lengths ρ (see Note 1 at end of text), embedded in a medium of density of coherent scattering lengths ρ_0, is given by the relation (Teixeira, 1992):

$$I(Q) = K \cdot P(Q) \cdot S(Q) \tag{1}$$

where $K = (\rho - \rho_0)^2$ is the contrast, $P(Q)$ the form factor of each particle, and $S(Q)$ the structure factor, which is related to the spatial distribution of the centers of mass.

Incoherent inelastic neutron scattering measurements and data analysis

The IINS experiments were performed on the MIBEMOL spectrometer at LLB. Inelastic neutron scattering spectroscopy is a standard tool in the investigation of the dynamics of solids and liquids (Lovesey, 1987) and involves measuring the velocity changes of neutrons after interaction with the sample. The exchange of energy $\hbar\omega$ and transfer momentum $\hbar Q$ can be related to time-correlation functions of the atomic motions in the sample. In such a scattering experiment we measure a neutron scattered intensity that is proportional to the double differential scattering cross-section expressed by the following relation:

$$\partial^2\sigma/\partial\Omega\partial\omega = \frac{k}{k_0} N \frac{\sigma_{\text{inc}}}{4\pi} S_{\text{inc}}(Q, \omega) \tag{2}$$

Here **Q** is defined as $\hbar\mathbf{Q} = \hbar(\mathbf{k} - \mathbf{k}_0)$, where **k** and $\mathbf{k}_0$ are, respectively, the scattered and incident neutron wavevectors; *Q* is the scattering vector modulus; $S_{\text{inc}}(Q, \omega)$ is the self-dynamic structure factor; and σ_{inc} the incoherent scattering cross-section. $S_{\text{inc}}(Q, \omega)$ can be decomposed into two contributions, a first one centered at $\omega = 0$ (including elastic and quasi-elastic terms) and a second one including inelastic contributions so that:

$$S_{\text{inc}}(Q, \omega) = S_{\text{elas}}(Q, \omega = 0) + S_{\text{quasi}}(Q, \omega) + S_{\text{inelas}}(Q, \omega) \tag{3}$$

The elastic peak arises from neutrons that are scattered with no change in energy, the quasi-elastic scattering appears as a more or less broad continuous band centered at $\omega = 0$ and arises from rotational or translational diffusive motions, and the inelastic scattering arises from transitions of the system between well-defined energy levels that are related to the vibrational modes of the system. Neutron scattering measurements were carried out at 298 K using neutrons at 6 Å wavelength with a resolution *R* of 96 μeV (defined as the full width at half-maximum of a vanadium standard). The covered *Q* range was 0.32–1.93 $Å^{-1}$. The measured time-of-flight spectra were corrected and normalized by adapted standard routines available at LLB. Due to the high transmission of the samples (95–97%), the spectra were not corrected for multiple scattering.

NMR measurements

Natural-abundance solid-state ^{13}C-NMR measurements were carried out on a Bruker CXP 400 NMR spectrometer (Bruker GmbH, Karlsruhe, Germany) under conditions of cross-polarization (CP), proton-decoupling, and magic-angle spinning (MAS), at Laboratoire des Mesures Physiques (University II, Montpellier, France). Approximately 40–50 mg of lyophilized protein at different levels of hydration (Fig. 6) were filled into a zirconium oxide cylindrical rotor. The samples were spun at the magic angle in the double-bearing 4 mm wide-bore system of the Bruker probe head at spinning speeds between 6 and 10 kHz. All spectra reported here are at a rotor frequency of 6.5 kHz, a value compatible with low temperatures under the conditions used. The FID was detected for 33 ms under proton decoupling at 400 MHz. The ^{13}C spectral width was 31 kHz, corresponding to 308 ppm with a carrier frequency of 100.62 MHz. The decoupler offset was set to the middle of the proton spectrum. Typically, 1600 FIDs were accumulated with 2048 points, zero-filled up to 4096 points, and then Fourier-transformed with no previous exponential multiplication. The mixing time under adjusted Hartman-Hahn conditions was 1 ms and the recycle delay between pulses was 5 s. Different recycle delays had no influence on the spectra. The 90° pulse time for ^{1}H was 4 μs. No attempt was done to favor carbons that undergo inefficient polarization transfer by recording the spectra without cross-polarization due to the loss of sensitivity and longer acquisition times. No special pulse sequence was used to eliminate the sidebands due to rotor spinning (see Fig. 6). The assignment of resonances in the solid-state ^{13}C-NMR spectra is based on the assumption that the MAS averaged chemical shifts coincide with those observed in the liquid state (Alattia et al., 1996). A chemical shift of 41.9 ppm was adopted for the center of the unique peak encompassing the 17 Lys $^{13}C_\epsilon$ resonances (internal reference) in the NMR spectrum of the most hydrated parvalbumin sample used ($h = 0.38$; see Fig. 6) and it corresponds to the mean value of the resolved chemical shifts in the liquid state with respect to the internal reference, sodium 3-trimethyl-silyl-(2,2,3,3-$^2H_4$)propionate or TSP-d4 (Alattia et al., 1996).

Calorimetric measurements

Measurements were performed on a DSC-7 differential scanning calorimeter (DSC) from Perkin-Elmer Corporation (Microanalytical Department, Norwalk, CT). About 10 mg of sample were sealed in an aluminum can. The low hydrated sample ($h = 0.15$ g/g) was hydrated by absorption of atmospheric water. The other hydrated samples were obtained by adding water directly on the powder to reach the desired hydration level or the desired concentration, in the case of the 20 mM solution.

RESULTS

Structural characterization of the powdered parvalbumin samples

SANS measurements

To characterize the powdered samples, SANS experiments were performed on parvalbumin powders at different hydration levels, as presented in Fig. 1. The dry protein ($h =$

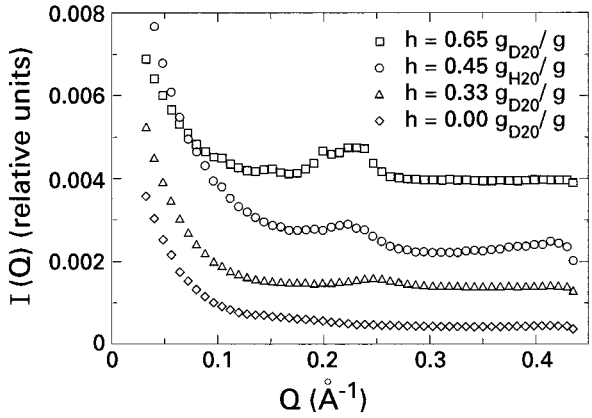

FIGURE 1 Small angle neutron scattering spectra of the fully Ca^{2+}-loaded form of parvalbumin powder as a function of hydration. Note that the circles are relative to an H_2O hydrated sample while the other samples have been hydrated by D_2O.

0) displays an $I(O)$ profile versus Q with a monotonous decrease of the scattered intensity with a small bump at 0.15 $Å^{-1}$. Similarly, the profile at $h = 0.33$ decreases monotonously at increasing Q values with a small bump shifted to 0.25 $Å^{-1}$. In contrast, the hydrated protein (at $h \geq 0.45$) displays a second peak centered at $\sim$0.22 $Å^{-1}$. The estimated density of the powder is of the order of 0.2 g/cm^3. The powder is therefore essentially made of voids and can be considered as a porous system. The intense scattering observed at Q values <0.1 $Å^{-1}$ is thought to be due to the scattering of the large pores produced by the voids. Following Eq. 1, the peak at 0.22 $Å^{-1}$ may have two origins: either a peak of the structure factor, $S(Q)$, due to the presence of a characteristic length between protein molecules, or a peak of the form factor of the molecule, $P(Q)$. The latter could be one of the interference peaks of the form factor $P(Q)$ in Eq. 1, of a shell of heavy water around the hydrogenated protein, the contribution of the peak being enhanced by the large contrast resulting from this isotopic effect. However, when the protein was hydrated with light water, i.e., in the absence of contrast (see Eq. 1) between the hydration shell and the protein, the peak is still present, as shown in Fig. 1. The peak is therefore evidence of a spatial correlation between particles of diameter $2\pi/0.22 = 29$ Å. Following Halle et al. (1981), the parvalbumin shape is reasonably described by a 15 Å radius sphere. We conclude that in the hydrated powders studied in this work (h values up to 0.65) the protein molecules are spatially very close to each other. In solution, a hydrodynamic radius of 22 Å was calculated from depolarized light scattering and nuclear resonance measurements (Bauer et al., 1974). This radius is $\sim$5 Å larger than the average crystallographic radius indicating that a significant amount of water is firmly bound to the protein in solution.

Solid-state ^{13}C-NMR measurements

A temperature-dependent NMR experiment was carried out with the aim to characterize the conformational features of the protein in its dry state. It is known from ^{1}H-NMR studies in solution that parvalbumin undergoes a conformational change in the 80°C range due to the undoing of its hydrophobic core (Parello et al., 1974; Cavé and Parello, 1981). As shown in Fig. 2, the CP-MAS ^{13}C-NMR spectrum of dry $PaCa_2$ remains practically unaltered within a large temperature range from 160 to 383 K. This is a striking observation that suggests a complete invariance of the protein structure, at least concerning the gross features of the structure, since the resolution achieved here on the solid-state CP-MAS ^{13}C-NMR spectra of parvalbumin is far from being comparable to the resolution obtained by ^{13}C-NMR in solution (Nelson et al., 1976). As presented below, none of the five Ile $^{13}C_\delta$ resonances is resolved in the solid-state spectrum (unique signal centered at 14.10 ppm (peak 1) in the spectrum of $PaCa_2$ at $h = 0.38$; see Fig. 6 *C*), although the isotropic chemical shifts of the resonances are separated by 0.75 ppm in solution (75 Hz at the observation frequency of 100 MHz). Similarly, the unique peak centered at $\sim$139 ppm in the solid-state spectrum (Fig. 6) contains the 9 Phe $^{13}C_1$ resonances, whereas in solution this region of the ^{13}C-NMR spectrum shows several resolved peaks (Nelson et al., 1976). Therefore, subtle structural rearrangements, if they occur, in the powdered protein as a function of temperature might remain unnoticed. In contrast to the spectral invariance observed with the dry powder as a

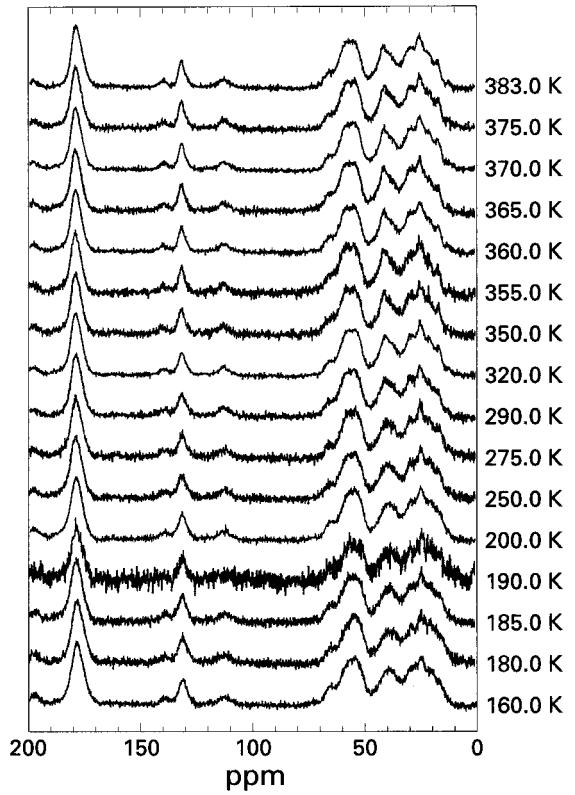

FIGURE 2 Proton decoupled natural-abundance 100 MHz CP-MAS ^{13}C-NMR spectra of the fully Ca^{2+}-loaded form of parvalbumin in the dry state in the temperature range 160–383 K. For the identification of the spinning sidebands see Fig. 6.

function of temperature (Fig. 2), marked spectral effects are observed on the solid-state ^{13}C-NMR spectra of powdered parvalbumin as a function of hydration at a constant temperature of 295 K (see Results below and Fig. 6). This is the case of the 10–50 ppm high-field region of the solid-state ^{13}C-NMR spectrum with several peaks (labeled 1–4 in Fig. 6) which all are sensitive to hydration (narrowing effects upon increase of hydration). The 41.9 ppm peak that corresponds to the 17 Lys $^{13}C_\epsilon$ resonances of the protein is the most affected by hydration. In contrast to its relative invariance upon temperature variation in the dry state, the lineshape of the 41.9 ppm peak becomes temperature-dependent provided the protein is sufficiently hydrated (note, however, that a narrower component is observed in Fig. 2 at 41.9 ppm for temperatures above 350 K). At $h = 0.21$, the Lys $^{13}C_\epsilon$ peak is definitely dependent on the temperature and is significantly sharpened above 350 K (NMR data not shown) in a manner similar to what is observed when hydration is increased from 0.21 to 0.38 but at a constant temperature of 295 K (see Fig. 6).

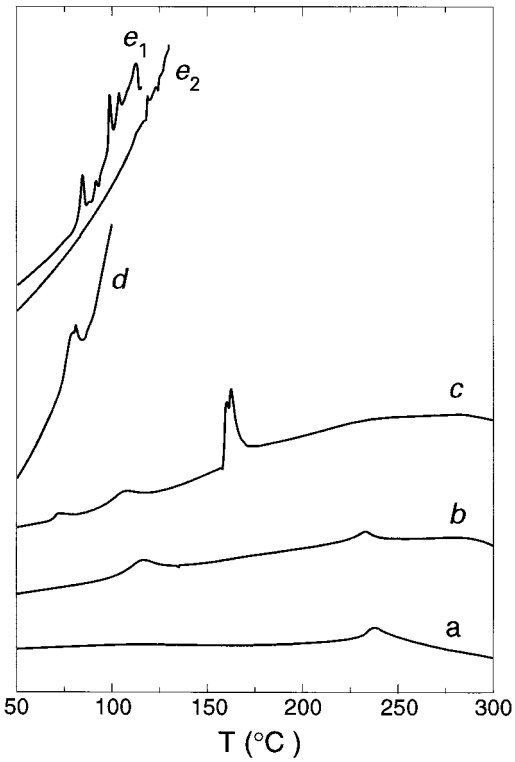

FIGURE 3 Thermograms of parvalbumin as a function of hydration level (H_2O hydrated samples), from the dry powder (*a*) to the solution. The differential scanning calorimetry (DSC) scans of the intermediate hydration levels are shown: $h = 0.15$ (*b*), $h = 0.64$ (*c*), $h = 0.85$ (*d*). The (e_1) and (e_2) profiles are relative to two successive scans performed on a 20-mM parvalbumin solution. We checked that all the transitions were irreversible; in particular, this is the case for the transitions observed on the 20-mM sample, as shown by the differences in the (e_1) and (e_2) scans. Note that the transition at 160°C for the sample hydrated at $h = 0.64$ is spurious, probably due to the explosion of the DSC cell at this temperature. The measured quantity is the differential heat flux between the sample and an empty can (in relative units homogeneous to watts). The thermograms were obtained upon heating starting from ambient temperature, with a scan rate of 20°C/min.

Calorimetric measurements

To further characterize the protein as a powder, DSC experiments were performed at different hydration levels in the 50–300°C range, as presented in Fig. 3. No heat transition was observed with the dry powder with the exception of a transition at ~235°C (Fig. 3, profile *a*) which is likely to correspond to the thermal decomposition of the protein as an organic compound. This result is in agreement with the aforementioned spectral invariance by solid-state ^{13}C-NMR spectroscopy at temperatures below 110°C (see Fig. 2). At partial hydration, $h = 0.15$, a heat transition is observed at ~100°C while the high-temperature transition (~230°C) is still present (Fig. 3 *b*). At higher hydration ($h = 0.64$) exceeding a monolayer coverage (see below), several heat transitions are observed: a major (composite) one at ~160°C, and two minor ones at ~110°C and ~70°C, respectively; we note, however, that the composite transition at ~160°C is spurious, as probably due to the explosion of the DSC cell at this temperature (Fig. 3 *c*). At higher hydration ($h = 0.85$), the low-temperature transition is shifted to ~80°C (Fig. 3 *d*) and finally it appears at ~85°C in the 20 mM solution (Fig. 3; profile e_1). Previous ^{1}H-NMR results on the thermal stability of parvalbumin in solution (Cavé and Parello, 1981), showed the occurrence of a conformational transition at 80–85°C which essentially involves the loss of the integrity of the hydrophobic core as inferred from the loss of the ring current-induced chemical shifts in the native state. It is likely that such a profound rearrangement of the protein tertiary structure while the secondary structure (six helical segments in the native state) is not essentially affected (Cavé et al., 1979a) gives rise to the thermal transition observed here by DSC with the hydrated parvalbumin sample, at $h > 0.6$. Interestingly, in the 20 mM solution, additional thermal transitions are observed on the DSC profile (e_1; Fig. 3) in the 90–115°C range and they could correspond to the undoing of the secondary structure elements (α-helices). Since we will not further address the question of the structural integrity of our powdered parvalbumin samples in the Discussion section, we conclude here that the occurrence of several DSC transitions in the hydrated powder (at $h > 0.65$) in register with temperature-induced structural transitions known to occur in solution provides strong evidence that a lyophilized parvalbumin sample retains the gross features of the native tertiary structure, although it markedly differs from the solution structure through its dynamical properties (see Discussion).

Finally, our DSC measurements allow us to define the total hydration value of parvalbumin by defining the amount of water that yields a thermal transition at 0°C due to the occurrence of free water yielding ice. The 0°C transition is observed at $h = 0.38$ (data not shown), whereas it is absent at h values below 0.35 in the DSC profiles. If we calculate

the accessible surface of parvalbumin as being 5930 Å^2 according to Miller et al. (1987) and if we assume that a water molecule occupies ~20 Å^2 of the protein surface (Rupley and Careri, 1991), we find that ~300 water molecules are required to form a "continuous" monolayer of water molecules corresponding to $h = 0.45$.

Hydration-coupled dynamics in parvalbumin

Quasi-elastic neutron scattering

The central part of the self-dynamic structure factor (Eq. 3) is analyzed as the sum of elastic and broadened terms according to:

$$S_{inc}(Q, \omega) = \exp(-Q^2\langle u^2\rangle/3)[(p + (1 - p)A_0(Q))\delta(\omega) + (1 - p)(1 - A_0(Q))L(Q, \omega)] \quad (4)$$

The exponential term is the Debye-Waller factor. We introduce a fraction p of immobile protons (at the resolution of the spectrometer), that contribute to the elastic part of the spectra $\delta(\omega)$. The $(1 - p)$ mobile protons undergo diffusive motions responsible for the quasi-elastic signal $L(Q, \omega)$ and contribute to the elastic intensity via the elastic incoherent structure factor (EISF), $A_0(Q)$. The experimental EISF is thus:

$$EISF(Q) = p + (1 - p)A_0(Q) \quad (5)$$

This latter term describes the time-averaged spatial distribution of the molecules (Bée, 1988). The second term of Eq. 4 is considered to be a Lorentzian line $L(Q, \omega)$ with a half-width at half-maximum Γ. Fig. 4 presents the elastic and quasi-elastic components of a typical time-of-flight IINS spectrum (see Materials and Methods) of $PaCa_2$, after hydration of the protein with D_2O (protein sample labeled $PaCa_2HHd$; see Materials and Methods) at $h = 0.31$. The fitting of the quasi-elastic component is based on Eq. 4, using a delta function and a single Lorentzian line. As shown in Fig. 5, *A* and *B*, the half-width at half-maximum of the Lorentzian line is plotted as a function of Q^2, at two different h values, i.e., 0.31 and 0.65, respectively. The invariance of Γ as a function of Q^2, at $h = 0.31$ (the same trend is observed for the dry sample and sample hydrated at $h = 0.12$; not shown), is to be interpreted as the result of

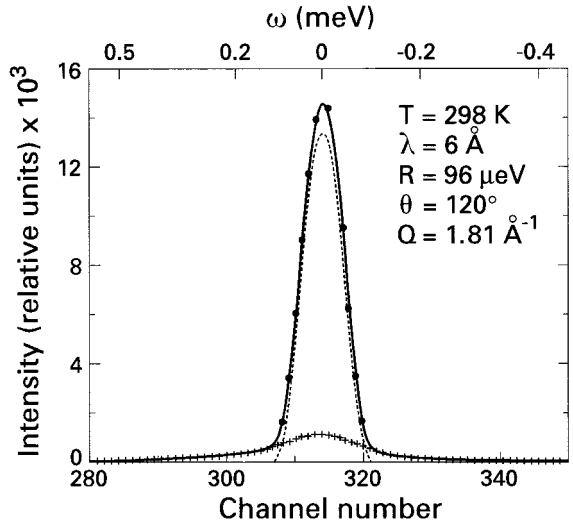

FIGURE 4 Elastic and quasi-elastic components of a neutron scattering time-of-flight spectrum at 6 Å wavelength, and 298 K of a parvalbumin $PaCa_2HHd$ sample hydrated at $h = 0.31$ g D_2O/g dry protein. *R* is the energy resolution. The filled circles are the experimental points; the solid line is the model fit (see Eq. 4).

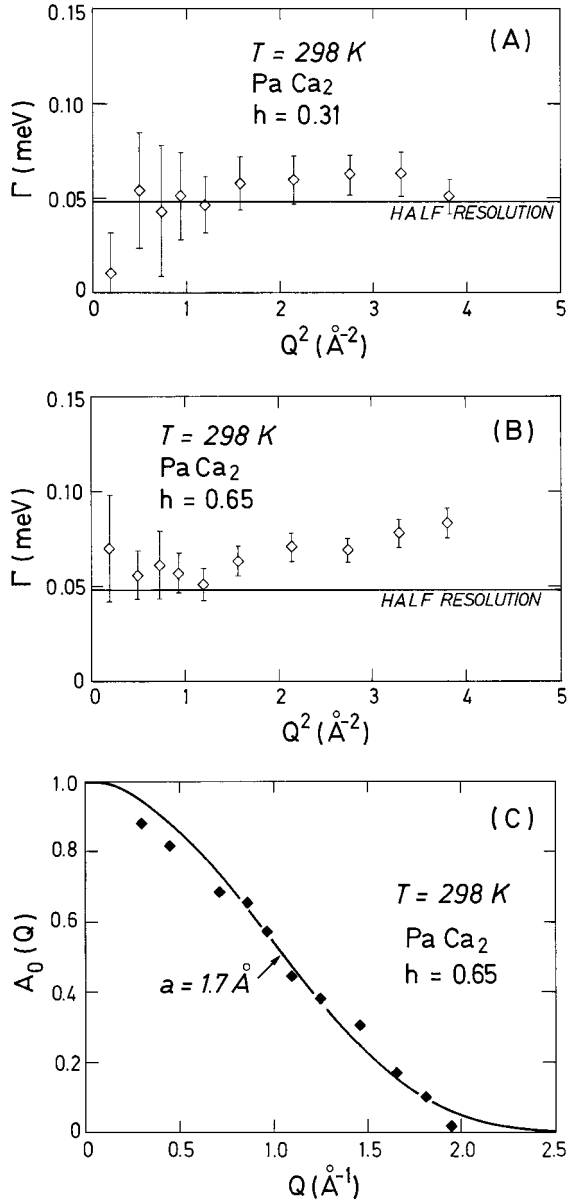

FIGURE 5 (*A*) Variation of the half-width at half-maximum of the Lorentzian line versus Q^2 for a parvalbumin $PaCa_2HHd$ sample hydrated at $h = 0.31$ g D_2O/g dry protein; (*B*) same conditions with the exception that $h = 0.65$ g D_2O/g dry protein; (*C*) Variation of the elastic incoherent structure factor, $A_0(Q)$, of the fraction $1 - p = 0.28$ of mobile protons in the protein versus Q using the data in (*B*); experimental points (*filled diamonds*), and model fitting (*solid line*) according to Eq. 6. All measurements are performed at 298 K.

reorientational motions of some of the protons in the protein, at the observation time scale of 10 ps. From the average value of Γ, we can deduce a correlation time $\tau = \hbar/\Gamma$ of 17, 13, and 11 ps at $h = 0$, 0.12, and 0.31, respectively.

At higher hydration ($h = 0.65$), Γ follows a plateau from 0.2 to 1.2 $Å^{-2}$, and becomes Q^2-dependent at higher Q^2 values. This is a characteristic feature of diffusion in a confined volume. According to the model of Volino and Dianoux (1980), the EISF of a particle diffusing in a sphere of radius a is:

$$A_0(Q) = \left(\frac{3j_1(Qa)}{Qa}\right)^2 \quad (6)$$

Where $j_1(x) = (\sin(x) - x\cos(x))/x^2$ is the spherical Bessel function of the first kind. For the data at $h = 0.65$, a quantitative treatment, using Eqs. 5 and 6 of the variation of the EISF as a function of Q, shows that $p = 0.72 \pm 0.2$ and $a = 1.7 \pm 0.1$ Å. This leads to the conclusion that ~30% of the protein protons diffuse in a volume that can be assimilated to a sphere with a radius of $a = 1.7$ Å. The elastic incoherent structure factor of those $(1 - p)$ mobile protons, $A_0(Q)$, is presented in Fig. 5 *C* as a function of Q. Following Volino and Dianoux (1980), the diffusion coefficient of the mobile protons ($D = 0.68 \cdot 10^{-5}$ cm^2/s), has been estimated from Γ_0, the limit of Γ at $Q = 0$ ($\Gamma_0 = 4.33 \cdot D/a^2$).

NMR lineshape studies

The CP-MAS ^{13}C-NMR spectra of $PaCa_2$ at different hydration levels up to near-monolayer coverage are shown in Fig. 6 (samples used $PaCa_2$HHh; See Materials and Methods). The main differences between the dry and the hydrated protein include a narrowing of several peaks in the high-field region of the spectrum (10–50 ppm). Among them the peaks labeled 1–4 undergo the more prominent changes at increasing hydration. Based on the liquid-state chemical shifts (Alattia et al., 1996), peaks 1–4 in the solid-state NMR spectra are assigned to the resonances of Ile$^{13}C_\delta$, Ala$^{13}C_\beta$, Lys$^{13}C_\delta$, and Lys$^{13}C_\epsilon$, respectively. Each peak is composite based on the amino acid composition of pike 5.0 parvalbumin, which includes 5 Ile, 19 Ala, and 17 Lys residues. These peaks were selected for assessing the motional features of the protein upon hydration.

Lysyl side chains. The sharpening of peaks 3 and 4 at increasing hydration is likely to result from a reduced distribution of the individual (isotropically MAS averaged) chemical shifts and/or from an enhancement in local mobility of the Lys side chains in comparison to the dry state. As shown in Fig. 7, the positive peak centered at 41.9 ppm on the difference spectrum "$h = 0.38$ − dry protein" is satisfactorily accounted for by the distribution of the liquid-state chemical shifts (from Alattia et al., 1996; see upper part of Fig. 7 and legend), thus suggesting that the distribution of chemical shifts in the MAS-averaged solid-state ^{13}C-NMR spectrum of hydrated $PaCa_2$ is closely related to the distribution of chemical shifts in the liquid state (see Discussion). Due to severe overlapping within the 40–45 ppm region from additional resonances besides the 17 lysyl $^{13}C_\epsilon$ ones, the lineshape of the latter (including a possible spreading in the distribution of isotropic chemical shifts) cannot be defined in the spectrum of the dry protein (Fig. 6 *A*).

Alanyl and isoleucyl side chains. A relatively sharp peak centered at 18.0 ppm (peak 2) is apparent in the CP-MAS ^{13}C-NMR spectra of parvalbumin at $h > 0.2$ (Fig. 6, *B* and *C*), whereas only a broad, unresolved, resonance is observed in the spectrum of the dry protein in this region of the

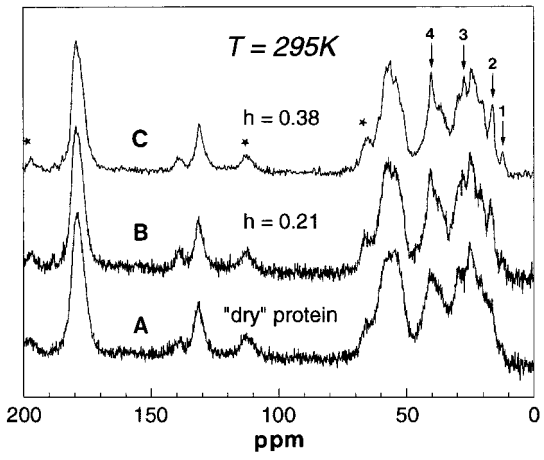

FIGURE 6 Solid-state proton-decoupled ^{13}C-NMR spectra at 100 MHz under cross-polarization, and magic-angle spinning conditions of parvalbumin $PaCa_2$HHh samples hydrated with normal water at (*A*) $h = 0$ or "dry sample," (*B*) $h = 0.21$, and (*C*) $h = 0.38$. Hydration values h are in g H_2O/g dry protein. Based on the liquid-state isotropic chemical shifts (Alattia et al., 1996), peaks labeled 1–4 are respectively assigned to the resonances of Ile$^{13}C_\delta$ (14.1 ppm), Ala$^{13}C_\beta$ (18.0 ppm), Lys$^{13}C_\delta$ (29.2 ppm), and Lys$^{13}C_\epsilon$ (41.9 ppm). All measurements were performed at 295 K. Spinning side bands (⋆) not suppressed.

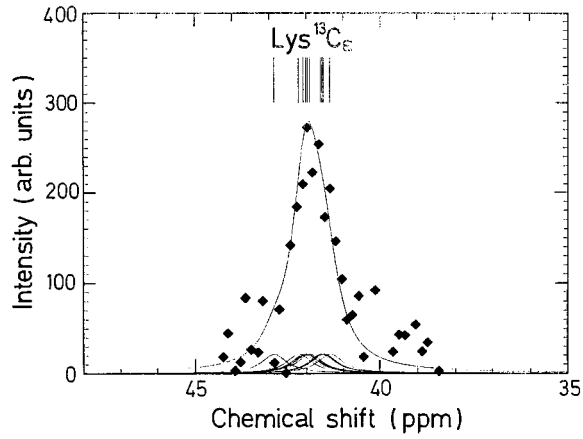

FIGURE 7 Difference between the solid-state ^{13}C-NMR spectrum of $PaCa_2$HHh, at $h = 0.38$, and the spectrum of the dry protein (see data in Fig. 3). Vertical bars account for the liquid-state isotropic chemical shifts of the individual Lys ^{13}C resonances (from Alattia et al., 1996). The model fit corresponds to the sum of Lorentzian lines assuming a common half-width for each individual resonance (see Results).

spectrum (Fig. 6 *A*). Based on the liquid-state chemical shifts (Alattia et al., 1996), it is concluded that at least 17 Ala^{13}C resonances, among 19 in total, contribute to the peak centered at 18.0 ppm in the solid-state NMR spectra of the hydrated protein. The difference spectrum, "$h = 0.38$ − dry protein," yields a positive peak at ~18 ppm (not shown), in agreement with the distribution of the liquid-state Ala C_β chemical shifts. Finally, the lineshape of the composite peak centered at 14.1 ppm (peak 1) with possibly five Ile methyl $^{13}C_\delta$ is also significantly dependent on protein hydration, as seen upon comparison of the three NMR spectra in Fig. 6.

Side chain dynamics. From the difference profile "$h = 0.38$ − dry protein" (Fig. 7), an averaged half-width value, at half-height, of 40 ± 6 Hz was inferred, giving the best fit for the experimental difference by using a sum of Lorentzian lines with each line having the chemical shift of a given individual Lys $^{13}C_\epsilon$ resonance in solution (from Alattia et al., 1996). Such a half-width would correspond to a transversal relaxation time T_2 of 16 ms if no broadening effects occur other than the ones due to spin-spin relaxation. However, it is known that under MAS conditions additional broadening effects are observed in the solid-state ^{13}C-NMR spectra due to residual dipole-dipole interactions (Komoroski, 1986) so that the T_2 value inferred from the lineshape of an individual lysyl $^{13}C_\epsilon$ resonance certainly corresponds to a lower limit. As previously described (Nelson et al., 1976), relaxation measurements in natural-abundance ^{13}C-NMR spectra are particularly adapted for a quantitative analysis of the underlying motions. This is due to the fact that for carbons with directly bonded hydrogens, the dominant relaxation mechanism is dipolar and the largest contribution to relaxation is from the bonded hydrogen. An estimated isotropic correlation time of ~20 ns was thus calculated from the T_2 value of 16 ms associated with the reorientation of the Lys $^{13}C_\epsilon$-^{1}H vectors according to a standard treatment (see Komoroski, 1986). Isotropic correlation times in the 20–30 ns were also calculated from the lineshapes of the Ala $^{13}C_\beta$ and Ile $^{13}C_\delta$ resonances (from similar difference profiles, as in Fig. 7, corrected for the distribution of isotropic chemical shifts in the hydrated state, $h = 0.38$).

DISCUSSION

Structural and dynamical features of powdered parvalbumin

The dry state

As a first goal of our study with powdered $PaCa_2$, we investigated the conformation of the dehydrated sample for which no structural data are available, in comparison to the structure of $PaCa_2$ in crystals and in solution. The invariance of the solid-state ^{13}C-NMR spectra of dry parvalbumin as a function of temperature (Fig. 2), as well as the absence of any thermal transition below 220°C by DSC (Fig. 3), suggest the existence of a highly structured protein for dry $PaCa_2$ that only differs from the native structure (as defined in the crystal form or in solution; Declercq et al., 1995; Padilla et al., 1988) by its restricted internal dynamics rather than by its gross structural features. However, strictly speaking, such an invariance based on the aforementioned techniques does not tell us whether the dry form of $PaCa_2$ possesses a tertiary fold close to the native one or is partially, if not totally, denatured. In the absence of any possibility to determine the "dry" structure at atomic resolution, we need to consider the variability of the structure upon hydration as performed in our work.

One criterion to assess the occurrence of a native-like structure in dehydrated parvalbumin comes from the work of Nelson et al. (1976) using high-resolution ^{13}C-NMR with $PaCa_2$ in solution. These authors described the occurrence of a one-carbon signal at 184.6 ppm (see Note 2) which was attributed to the invariant Glu-81. Its low-field position in comparison to the other carboxylate groups (from Asp and Glu) is explained by the presence of a salt bridge (carboxylate-guanidinium) between Glu-81 and Arg-75 (Kretsinger and Nockolds, 1973). Similarly, the single carbon of the guanidinium group of Arg-75 was identified as one-carbon resonance at 158.8 ppm (Opella, 1975). We note the presence of a weak ^{13}C peak at ~188 ppm in the solid-state ^{13}C-NMR spectrum of $PaCa_2$ (see Fig. 6 *C*), which is tentatively identified with the carboxylate ^{13}C resonance of Glu-81. Similarly, a weak signal at 160.5 ppm is observed with $PaCa_2$ at $h = 0.38$ (see Fig. 6 *C*). If both signals at ~188 and 160.5 ppm in the CP-MAS spectrum of $PaCa_2$ are not artifacts (a more careful analysis of the solid-state ^{13}C-NMR spectra of parvalbumin is required in this respect), their presence strengthens our conclusion that the dry or partially hydrated parvalbumin powders retain a native conformation. Indeed, the Glu-81–Arg-75 salt bridge is an invariant feature of the parvalbumin tertiary structure (Kawasaki and Kretsinger, 1994). Furthermore, based on x-ray crystallographic evidence this salt bridge is hydrated on one face, whereas the other face is directed toward the protein interior (Declercq et al., 1991; Roquet et al., 1992 and references therein) and this could explain that these one-carbon resonances are observed at partial hydration (see Fig. 6 *C*).

Another criterion in favor of a structured dry $PaCa_2$ protein is provided by the DSC profiles at increasing hydration (Fig. 3). These calorimetric studies with hydrated $PaCa_2$ powders (h from 0 to 0.85), as well as with a 20 mM solution, show that hydration markedly affects the thermal behavior of the protein. At $h = 0$, the protein shows no thermal transition besides a high temperature one at ~230°C (Fig. 3, profile *a*), in agreement with the solid-state ^{13}C-NMR data with $PaCa_2$ (Fig. 2). The observation of a thermal transition at ~115°C for $PaCa_2$, at $h = 0.15$ (besides the high-temperature one already observed at $h = 0$), clearly indicates that the protein acquires some mobility upon hydration. At higher hydration, i.e., $h = 0.64$ and 0.85, the thermal transition at 100–110°C is still observed, whereas a novel transition is observed in the 70–80°C region of the thermogram. In the 20 mM solution the latter

is shifted to 85°C. This thermal transition coincides with a conformational transition that was initially reported in solution based on high resolution ^{1}H-NMR (Parello et al., 1974; Cavé and Parello, 1981). This conformational transition, which depends on the ionic composition of the solution, occurs at 80–85°C at low ionic strength (Cavé and Parello, 1981), in complete agreement with the DSC results reported here with $PaCa_2$ dissolved in water. The 85°C NMR transition was attributed to the unfolding of the hydrophobic core of parvalbumin (Cavé and Parello, 1981) without significantly affecting the protein secondary organization (Cavé et al., 1979a). It is interesting to note that the DSC experiment with $PaCa_2$ in solution (see Fig. 3: profile e_1) shows a series of resolved thermal transitions between 90 and 110°C.

This composite region of the thermogram could correspond to the melting of the different helical segments of the protein (six in total, i.e., helices A–F; Kawasaki and Kretsinger, 1994) before a fully denatured state is obtained. The $PaCa_2$ form of parvalbumin apparently offers an example of a sharp dichotomy between the thermal stability of its tertiary folding (hydrophobic core) and the stability of its secondary structure. In conclusion, the fact that upon increasing the hydration of powdered $PaCa_2$, the DSC thermograms progressively approach the thermal behavior of the protein in solution can be considered as strong evidence that the lyophilized protein (dehydrated; residual or constitutive water molecules still present; see Materials and Methods) protein adopts a native-like structure. In agreement with this conclusion, the DSC profiles are irreversible once the protein has been denatured. Also in agreement with our conclusion that dry and partially hydrated $PaCa_2$ powdered samples display a native-type conformation, we note here the initial work of Jardetzky and Wade-Jardetzky (1980) who used a combination of high-resolution solid-state and solution ^{13}C-NMR to compare the structures of lysozyme in both states, in crystals and in solution. These authors concluded that the conformations of the protein in both states are closely related, although such a conclusion only concerns the gross features of the structure but does not permit the observation or the exclusion of more subtle differences. We presently have no equivalent NMR spectrum in solution at the same observation frequency (100 MHz) of our CP-MAS solid-state ^{13}C-NMR spectrum to perform a detailed comparison between both states of pike 5.0 parvalbumin.

It is accepted that a dehydrated protein is "frozen" in a restricted set of taxonomic conformational substates (Frauenfelder and Gratton, 1986), if not a unique substate, so that movements in the nanosecond time scale and above, which are associated with energy barrier-dependent interconversions, are hindered, while motions in the picosecond time scale corresponding to local librations of diffusive origin can persist. Such a view is substantiated by our parallel study of dry $PaCa_2$ by IQNS and by solid-state ^{13}C-NMR. The absence of slow dynamics (with time scales from microseconds to milliseconds) in the dehydrated $PaCa_2$ sample accounts for the absence of the characteristic spectral features (*narrow lines*), which are observed on the ^{13}C-NMR spectra of the hydrated samples (compare Fig. 6 *A* with Fig. 6 *C*). One well-known dynamical feature of parvalbumin is the "fluidity" of its hydrophobic core in the nanosecond, as well as microsecond-millisecond, time scales as inferred from solution ^{13}C-NMR relaxation measurements (Nelson et al., 1976) and ^{1}H-NMR lineshape analyses (Cavé et al., 1976; Cavé and Parello, 1981), respectively. Our initial goal for carrying out the CP-MAS ^{13}C-NMR experiments at low temperature (see Fig. 2) was to investigate the dynamical state of the Phe rings in dry $PaCa_2$.

It is known that in solution (at temperatures above 0°C) the Phe rings of parvalbumin undergo flipping motions about their C_β-C_1 bonds with rates exceeding 10^3 s^{-1} based on a lineshape analysis of the one-dimensional ^{1}H-NMR spectra (Cavé et al., 1976; Cavé and Parello, 1981). Under these conditions, the five ^{1}H spin systems for each Phe ring in $PaCa_2$ give rise to a time-averaged spectrum with three resolved peaks of relative intensities 1 (for proton H_4), 2 (for protons H_2 and H_6), and 2 (for protons H_3 and H_4). The same rules will apply for the aromatic ^{13}C spins of Phe so that fast and slow flipping motions (on the NMR time scale) about the C_β-C_1 bonds will result in lineshape differences for carbons 2, 3, 5, and 6, while carbons 1 and 4 lying along the C_β-C_1 axis will remain unperturbed. The peak encompassing all aromatic carbons bearing a hydrogen atom (i.e., all aromatic carbons except the C_1 carbons) centered at ~132 ppm will thus be highly composite. As apparent in Fig. 2, no significant variation of the shape of the peak at 132 ppm was observed even at the lowest temperature used (160 K) during our variable temperature CP-MAS ^{13}C-NMR experiments. One explanation to account for such an invariance would be that the dry protein is sufficiently constrained dynamically (see above) so that the energy barriers between the Phe substates ($\pm 180°$ χ_2 rotamers) could be much higher than in the hydrated state and no interconversion is rapid enough on the NMR time scale, at any temperature, to average the spin systems. The 132 ppm peak will then include a series of nine spin systems with five nonequivalent ^{13}C resonances (slow exchange conditions on the NMR time scale). If this is the case, the distribution of isotropic chemical shifts will be rather narrow, since the peak at 132 ppm covers a spectral region of no more than 5 ppm in total (i.e., 500 Hz under the conditions used). So far the sequence-specific chemical shifts for the Phe aromatic carbons of pike 5.0 $PaCa_2$ in solution are not known (Alattia et al., 1996) and we only refer in this work to the assignments of Nelson et al. (1976) based on the chemical nature of each amino acid instead of sequence-specific assignments. If our interpretation is correct this would mean that in dry $PaCa_2$ no slow dynamics ($\pm 180°$ flipping motions of the Phe aromatic rings) are allowed. A systematic study of the dependence of lineshapes and relaxation parameters of the aromatic carbon resonances by solid-state ^{13}C NMR, as a function of temperature and hydration in powdered $PaCa_2$, needs to be carried out to assess or invalidate such a con-

clusion. It appears of the highest interest to monitor such slow dynamics events as a function of hydration if we consider the possibility of a coupling between internal dynamics in the millisecond time scale and the dissociation rates of the divalent cations bound to parvalbumin, as discussed below. Similarly, the absence of narrow peaks at $h = 0$, in contrast to what is observed at higher hydration values ($h > 0.2$) on the solid-state ^{13}C-NMR spectra (compare Fig. 6, *A* and *C*), can be interpreted as due to the absence of motions in the nanosecond time scale in dry $PaCa_2$. Indeed, as reported in Results, the narrow peaks, 1–4, in the hydrated protein (Fig. 6 *C*) are associated with motions in the 20–30 ns range (these values are likely to correspond to upper limits of the lifetimes; see above) and these peaks are absent in the dry protein (Fig. 6 *A*). A clear understanding of the nuclear relaxation mechanisms and molecular dynamics that govern the lineshapes in the solid-state CP-MAS ^{13}C-NMR spectrum of dry $PaCa_2$ would require a detailed analysis encompassing T_1 and T_2 measurements (in the laboratory and in the rotating frame), using isotopic labeling of selected amine acids.

With regard to the presence of internal motions in dehydrated ($h = 0$) $PaCa_2$, our studies by IQNS offer evidence for the occurrence of motions in the 1–10 ps time scale (see Fig. 5). The IQNS data with the dry ($h = 0$) and lowly hydrated ($h = 0.12$) protein are characterized by a weak quasi-elastic signal, with 71 being *Q*-independent (data not shown) in a similar manner as to that observed for the more hydrated sample at $h = 0.31$ (Fig. 5 *A*). This leads to the conclusion that these diffusive motions are reorientational in nature about scarcely hindered bonds and/or rotationally diffusive motions involving three (e.g., methyl group reorientation about the C_3 axis) or more sites. We therefore conclude that these movements in the dry and low hydrated states are characterized by longer correlation times than at higher hydration ($h = 0.31$ and 0.65). These motions originate exclusively from the protein since D_2O was used as the hydration water. No difference was also observed when a pre-exchanged sample, $PaCa_2$HDd (see Materials and Methods) with all its exchangeable protons substituted by deuterium atoms was used for the IINS experiments, thus corroborating our conclusion that the observed IQNS signal essentially originates from the contribution of the nonexchangeable protons in the protein.

Hydrated states

In the hydrated powdered $PaCa_2$ samples an extended repertoire of internal motions is at play, in comparison to the dry state, encompassing time scales in the picosecond-nanosecond range, as inferred from our parallel approach using neutron scattering and solid-state NMR. If slower motions in the picosecond-millisecond time scale are also present in these hydrated states, as is the case in solution (i.e., flipping motions of the Phe aromatic rings; see above), this remains an open question. The observation, however, of a selective variation in the dynamical regime of the internal Ile side chains upon hydration, as inferred from our solid-state ^{13}C-NMR study of pike 5.0 $PaCa_2$ at different hydration values (Fig. 6; see also Results), suggests that the hydrophobic core of powdered $PaCa_2$ becomes more mobile at increasing *h* values. It has been recently observed that $PaCa_2$ displays a relatively large set of conformational substates based on x-ray crystallographic data with the isoform from pike, pI 4.10 $PaCa_2$, at atomic resolution 0.91 Å and at low temperature 100 K (Declercq et al., 1999). These data show that 16 residues, among 108 in total, including polar external residues (Ser, Lys, Glu), as well as nonpolar internal residues (Phe, Val, Leu, Ile), display well-defined substates (designated A and B for each residue), thus accounting for at least 2^{16} distinct conformational substates in the protein (Declercq et al., submitted for publication, 1998). With regard to the hydrophobic core, two isoleucyl residues, i.e., the invariant Ile-50 and Ile-97, display two sets of such substates A and B, at low temperature, besides other internal residues. At 295 K it is likely that there is an equilibrium between these substates within the hydrophobic core, thus affecting the dynamics of this internal domain in a global manner. The observation that the isoleucyl side chains become more mobile upon hydration of the dry $PaCa_2$ powder, as inferred from our NMR study (see the evolution of the lineshape of peak 1 in Fig. 6), suggests that the hydrophobic core of $PaCa_2$ becomes more mobile upon hydration even at *h* values between 0.2 and 0.4 (see Note 3).

Interestingly, as apparent in Fig. 6, the sharpening of peak 1 (Ile) at increasing hydration follows that of peaks 3 and 4 (Lys), as well as that of peak 2 (Ala), thus suggesting that the mobility of the hydrophobic core is a late event in comparison to the induction of an increased mobility at the protein surface through water binding to accessible polar groups. This is a remarkable observation in the sense that it suggests a progressive induction of mobility from the periphery of the protein toward its interior upon increasing the degree of hydration. At $h = 0.2$, i.e., 128 water molecules per parvalbumin molecule, only a partial coverage of the protein surface is achieved (~300 water molecules are required for a complete coverage of the surface with a water monolayer; see Results). If one takes only into account the charged residues known to be externally located based on the crystal structure of pike 5.0 $PaCa_2$ (Declercq et al., 1995), i.e., 17 Lys, 9 Asp, and 7 Glu (all Asp and Glu residues involved in Ca^{2+}-coordination have been omitted), a total number of hydration water molecules from 83 to 115 can be considered depending on the stoichiometry of hydration of the different charged groups. As shown in Fig. 8 *C*, an ammonium polar group of Lys is surrounded by three water molecules at hydrogen bond distances in agreement with the occurrence of three hydrogen atoms on the nitrogen atom. These stoichiometric considerations suggest that at $h \sim 0.2$ most of the water molecules, if not all, are hydrating the charged groups at the surface of the protein. Above this *h* value of 0.2, the additional water molecules will start clustering around the initial hydration loci around the polar groups and thus establish a network of water molecules at

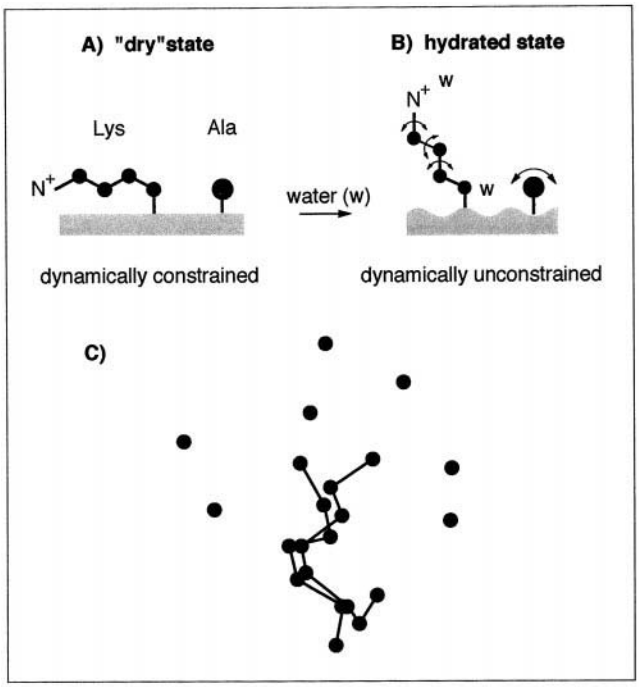

FIGURE 8 Schematic presentation of selected dynamical events induced by hydration of a globular protein as inferred from the neutron scattering and NMR study of parvalbumin at different hydration levels. (*A*) In the *dry state*, strong electrostatic interactions intervene in a low dielectric constant medium and contribute to rigidify the protein molecule. A lysyl (Lys) side chain adopts a "bent" conformation with its ammonium polar head interacting with protein anionic sites. The entire protein matrix (*stippled area*) is assumed to be highly constrained. (*B*) In the *hydrated state* ($h > 0.2$ g water/g dry protein), a Lys polymethylene side chain adopts an extended conformation, as a consequence of selective hydration of its ammonium polar head, thus allowing side chain motions to occur. Librations are indicated by curved double arrows at the level of the more exterior bonds, i.e., C_β-C_γ, C_γ-C_δ, and C_δ-C_ϵ. The combination of these rapid librations or partial rotations around the successive C-C bonds of a lysyl side chain results in a complex motion that accounts for the diffusion-type motions of hydrogen within a confined volume (see text) in the picosecond range, as inferred from the IQNS measurements. Hydration of polar elements at the protein surface are assumed to induce overall breathing motions in the protein (represented by the "undulating" surface) by softening the electrostatic interactions in the dry state. A short side chain, such as in alanine (Ala), could be dynamically coupled to such breathing motions of the protein, as inferred from the NMR measurements. The magnitude of the dots along the Lys and Ala side chains accounts for the number of protons (*small filled circle* = CH_2, *large filled circle* = CH_3) contributing to the IQNS signal. The symbol W indicates hydration water molecules. (*C*) An example of a two-state arrangement of a hydrated (external) lysyl side chain, i.e., Lys-91 in the crystal structure of pike 4.10 $PaCa_2$ determined at atomic resolution (0.91 Å) and at low temperature, 100 K (Declercq et al., submitted for publication). The two states essentially differ by their torsional angles for the single bonds close to the ammonium group. The surrounding dots (water oxygen atoms) correspond to well-defined water molecules in the crystal structure. Lys-91 is also present in pike 5.0 parvalbumin investigated here. (Fig. 8 *C* courtesy of J.-P. Declercq, Louvain-La-Neuve, Belgium).

the surface of the protein. This additional deposit of water molecules at the protein surface could be responsible for a general "softening" of the protein structure. Such a view is supported by the general trends observed in parallel by IQNS and ^{13}C-NMR in this work.

As stated above, parvalbumin in solution is characterized by a remarkable mobility of its hydrophobic core if one considers the occurrence of the Phe flipping motions that occur with frequencies of 1000 s^{-1} or above at ambient temperature (Cavé et al., 1976; Cavé and Parello, 1981). Presently, we have no evidence whether these characteristic dynamical events also occur in the hydrated $PaCa_2$ powders. The induction of an increased mobility at the level of the internal Ile side chains, at h above 0.2, suggests that the entire hydrophobic core will adopt a higher mobility at that degree of hydration. The absence of any prominent alteration of the lineshape of the ^{13}C aromatic resonances (125–140 ppm region of the CP-MAS ^{13}C-NMR spectrum in Fig. 6) upon hydration needs to be considered with some caution since several processes are possibly at play for shaping these Phe resonances: 1) an intrinsic dependence of the individual linewidths (T_2 relaxation) on hydration; 2) interconversions between energetically identical substates (for a review see Gurd and Rothgeb, 1979) whose rates could also be hydration-dependent. These processes could result in mutual canceling so that the lineshapes of the Phe resonances in the CP-MAS ^{13}C-NMR spectrum of $PaCa_2$ could remain practically unaltered upon hydration at 295 K, under a restricted set of experimental conditions, as given in Fig. 6. Since the spreading of chemical shifts for the different ^{13}C aromatic resonances in $PaCa_2$ does not exceed a few hundred hertz (under the experimental conditions used, i.e., 100 MHz for the observing frequency), any flipping motion with a rate above 100–500 s^{-1} will result in rapid exchange conditions on the NMR time scale, thus leaving the lineshapes essentially unaffected if the flipping rates remain higher than this frequency threshold, independently of the hydration state of the protein. This specific aspect of the internal dynamics of parvalbumin would require investigation in a detailed manner as a function of temperature and hydration by ^{13}C-NMR. There is no contradiction in considering that, in the dry state, the Phe flipping motions will be sufficiently hindered, whereas upon hydration, at $h >$ 0.2, the hydrophobic core will display an increasing degree of mobility as the one observed in solution. The expected line-sharpening of the aromatic ^{13}C resonances subsequent to the increase in the internal correlation times upon hydration could be canceled by a concomitant broadening due to chemical exchange with the Phe spin systems (for a more complete discussion see Gurd and Rothgeb, 1979).

Whereas at $h = 0.31$ the IQNS signal is invariant as a function of Q^2 up to $Q^2 = 4.0$ $Å^{-2}$ under our instrumental conditions (Fig. 5 *A*; see also Materials and Methods), at a higher hydration of $h = 0.65$ (exceeding a continuous monolayer of water molecules; see Results), the IQNS signal becomes clearly dependent on Q^2 above 1.5 $Å^{-2}$ (Fig. 5 *B*). This indicates that, under such conditions of hydration, diffusive motions of protons occur in the protein within a confined volume. The use of Eqs. 5 and 6 yields a fraction $p = 0.72$ of protons seen as "immobile" at the present energy resolution, so that the remaining protons in the protein, ~30%, are involved in diffusive motions in the 10

ps range and confined within a spherical domain of a 1.7 Å radius (see Fig. 5 *C*). In parallel, our solid-state ^{13}C-NMR study shows that at $h = 0.38$ (Fig. 6 *C*), a hydration level close to coverage by a monolayer of water molecules, the side chains of the lysyl residues appear dynamically unconstrained in comparison to the dry parvalbumin sample (Fig. 6 *A*). The 17 Lys side chains of pike 5.0 parvalbumin account for 136 nonexchangeable methylene hydrogen atoms of a total of 846 hydrogen atoms in the protein, i.e., 178 exchangeable (see Note 4) and 668 nonexchangeable. The lysyl side-chain hydrogen atoms thus represent as much as 20% of all nonexchangeable hydrogen atoms in the protein. This corresponds to a substantial population of hydrogen atoms that are likely to contribute to the IQNS signal through their hydration-dependent dynamical properties. Other hydrogen-containing side chains at the surface of the protein are also expected to contribute to the IQNS signal, such as Glu (with two methylene groups) and Asp (with one methylene group) since these residues are known to be primarily involved in the hydration process (Rupley and Careri, 1991). The side chains of Glu and Asp, taken together, involve 64 nonexchangeable hydrogen atoms, which could significantly contribute to the IQNS signal. Altogether, the population of nonexchangeable hydrogen atoms from Asp, Glu, and Lys represents as much as 30% of the total population of nonexchangeable hydrogen atoms present in our $PaCa_2HDd$ samples. This percentage apparently corresponds to the fraction $1 - p = \sim 30\%$ of mobile hydrogen atoms inferred from the experimental EISF values. However, based on the difference profile of Fig. 7, there is no real indication by solid-state ^{13}C-NMR that the abundant Asp side chains are dynamically affected upon hydration, although there is evidence by IR spectroscopy that hydration contributes to specific contacts with the carboxylate groups (Rupley and Careri, 1991). The hydration of charged groups in powdered proteins is almost complete at $h = 0.1$ corresponding to approximately two molecules of water per charge (Frauenfelder and Gratton, 1986). Most of the Asp $^{13}C_\beta$ resonances lie in the 39–41 ppm region of the MAS-averaged ^{13}C-NMR spectrum of pike 5.0 $PaCa_2$, with the exception of two high-field shifted $^{13}C_\beta$ resonances at 38.13 ppm and 38.37 ppm from Asp-42 and Asp-51, respectively (isotropic chemical shifts in solution from Alattia et al., 1996). Although variations in the shape of the Asp $^{13}C_\beta$ resonances could be obscured by the 17 Lys $^{13}C_\epsilon$ resonances (centered at 41.9 ppm; see Fig. 7), the number of Asp residues is large enough (14 residues in total) so that a possible hydration-induced narrowing of the Asp $^{13}C_\beta$ resonances could be readily detected if it does occur.

However, in parvalbumin, as in all EF-hand calciproteins, up to six polar residues (Asp, Glu, Ser) are involved in the direct coordination of the central cation in each EF-hand Ca^{2+}/Mg^{2+} binding site, as mentioned above. In pike pI 5.0 parvalbumin (this work) with two EF-hands, five aspartyl residues (D51, D53, D90, D92, D94) among 14 in total, one seryl residue S55 (among four in total) and two glutamyl residues (E62 and E101) among nine in total, are involved in the direct coordination of the two Ca^{2+} ions of $PaCa_2$, and are therefore only partially hydratable. The residual positive contribution in this 38–41 ppm region of the difference spectrum of Fig. 7 (right side of the lysyl $^{13}C_\epsilon$ resonances) could thus represent the contribution of the population of the nine external (hydratable) aspartyl residues in the protein. Presently, this assignment can only be tentative. Since an aspartyl side chain is a short one, with a single methylene group, in contrast to Lys with four methylene groups, it is possible that the torsional motions around the Asp C_α-C_β bonds (χ_1 rotamers) could be restricted due to steric hindrance effects with other closely lying elements of the protein. This is not the case for the long polymethylene lysyl side chains that protuberate from the protein structure with their amine groups exposed to the solvent (see Fig. 9). This could explain why the lysyl side chain ^{13}C resonances (specifically the C_ϵ and C_δ carbons) experience marked narrowing effects of their linewidths, whereas the aspartyl C_β resonances remain practically unaltered. This does not preclude, however, that in the first steps of the protein hydration, the charged carboxylate groups from Asp and Glu are also interacting with the added water molecules. It is well established through other physicochemical methods, including IR spectroscopy, that the carboxylic/carboxylate groups of Asp and Glu are hydratable in protein powders (Rupley and Careri, 1991).

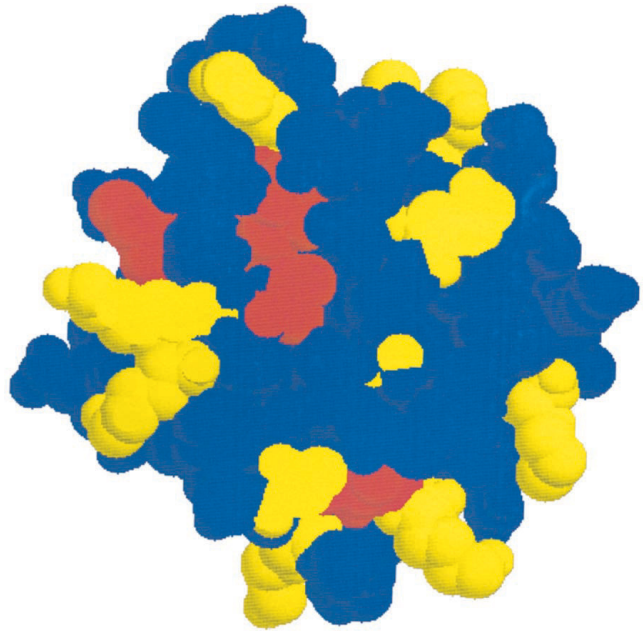

FIGURE 9 Space-filling model of the 1.65 Å crystal structure of pike 5.0 parvalbumin $PaCa_2$ (Declercq, J. P., B. Tinaut, F. Roquet, J. Rambaud, and J. Pavello. 1995. Protein Data Bank code entry 1PVA) shown as a cut displaying ~35% of the molecule (seen down the plane). Lysine residues are shown in yellow; isoleucyl residues are shown in red; all other residues are shown in dark blue. Isoleucyl residues: 1) the red trace in the bottom corresponds to Ile-11; 2) the central red cluster includes Ile-50, Ile-58, and Ile-97; 3) the peripheral red trace on the top left corresponds to Ile-99. The lysyl residues shown (8 among 17, in total) are not identified by their sequential positions.

Identification of selective hydration-dependent motions

The main goal of our study with hydrated parvalbumin powders combining IQNS and CP-MAS ^{13}C-NMR was to achieve a description of the effects of hydration on the internal dynamics of the protein at different timescales (picosecond and nanosecond, respectively), as well as to assess the origin of the chemical groups involved in such hydration-coupled motions. The observation that external, as well as internal, residues in $PaCa_2$ are dynamically affected by hydration, based on our solid-state ^{13}C-NMR study of parvalbumin (see Fig. 6 and Results), suggests that protein-water interactions that occur essentially at the protein surface (parvalbumin displays no buried water molecules within cavities), affect the protein dynamics not only at the level of the external side chains (lysyl residues), but also at the level of more internally located side chains from isoleucyl and alanyl residues.

Lysyl residues

As is apparent in Fig. 6 (see also Results), the most remarkable feature on the CP-MAS ^{13}C-NMR spectra of $PaCa_2$ is the marked sharpening of the Lys $^{13}C_\delta$ and $^{13}C_\epsilon$ resonances (peaks 3 and 4, at 29.2 and 41.9 ppm, respectively, in Fig. 6 *C*). No sharp signal for the Lys $^{13}C_\beta$ and $^{13}C\gamma$ resonances (at 31.4–33.4 ppm and 24–29 ppm, respectively; Alattia et al., 1996) is apparently detected upon hydration. This leads to the view that it is only the ammonium extremity of a given lysyl side chain, including the $C_\epsilon H_2$ and $C_\delta H_2$ methylene groups, which becomes highly mobile upon selective hydration of the ammonium polar head in contrast to the more internal part of the side chain. This view is well substantiated by the crystallographic results presented in Fig. 8 *C* in the case of Lys-91 (see legend to figure). As stated above (see Discussion), the abundant Lys side chains of pike 5.0 parvalbumin representing ~20% of the nonexchangeable hydrogen atoms of the protein will largely contribute to the IQNS signal. However, a given lysyl side chain cannot be considered dynamically homogenous, as inferred from the ^{13}C-NMR study of $PaCa_2$ at different hydration values, so that some of the loci along the polymethylene side chain will contribute preferentially to the IQNS signal within the time window available under the experimental conditions used. The ammonium extremity of the lysyl side chains, including the $C_\epsilon H_2$ and $C_\delta H_2$ methylene groups, could thus preferentially contribute to the IQNS signal in contrast to the more constrained part of the side chain including the $C_\beta H_2$ and $C_\gamma H_2$ methylene groups.

Alanyl residues

The case of the motions associated with the Ala residues is highly relevant to the mechanistic aspects of the internal dynamics in parvalbumin. The NMR probes monitoring these internal motions are the alanyl $^{13}C_\beta$-^{1}H vectors, which upon reorientation in the external magnetic field control the relaxation properties of the corresponding $^{13}C_\beta$ nuclei. The dynamics of Ala in proteins and Ala-containing model peptides have been analyzed in a rather detailed manner by ^{13}C-NMR (Henry et al., 1986), by neutron scattering (Drexel and Peticolas, 1975) and through theoretical simulations (Rossky and Karplus, 1979; Kneller et al., 1992). As shown by Henry et al. (1986), in the case of the detergent-solubilized coat protein of bacteriophage M13, the dynamics of the Ala residues based on ^{13}C-NMR relaxation are complex and translate motions about the C_α-C_β bonds, as well as motions from the main chain itself. The C_3 reorientations of the methyl groups of Ala occur in the picosecond range at ambient temperature in the case of Ala-containing peptide models. In poly-L-alanine, a torsional frequency of 230 cm^{-1} is observed by IINS (Drexel and Peticolas, 1975).

The selective sharpening of the Ala $^{13}C_\beta$ peak on the solid-state ^{13}C-NMR spectrum upon parvalbumin hydration (Fig. 6), is likely to involve a dynamical coupling between the Ala side chains and the protein backbone, which will allow the $^{13}C_\beta$-^{1}H vectors in the Ala methyl groups to display reorientational components in the nanosecond time scale. If hydration water controls the whole shape of the protein, as suggested by theoretical results (Steinbach and Brooks, 1993), then the C_3 rotations of the Ala residues, as well as the Ala motions coupled to the protein main-chain, will become less hindered through progressive hydration of the protein surface and hydration will generate a wide spectrum of motions detected by different spectroscopic techniques. In this respect the abundant Ala residues (19 in total in pike 5.0 parvalbumin) might contribute to the IINS spectrum, in the 1–10 ps time range, with 57 methyl protons in total, as well as to ^{13}C-NMR relaxation, in the nanosecond range. In their recent study on the internal dynamics of pike 5.0 parvalbumin $PaCa_2$ in solution by ^{13}C-NMR at natural abundance, Alattia et al. (1996) have inferred internal correlation times in the 1–70 ps range from the relaxation parameters of the α carbons (with a few carbons having larger internal correlation times of 162 ps for His-26 and 550 ps for His-107). Such motions could also be part of the dynamical repertoire of the hydrated parvalbumin powders. The Ala residues with most of the internal correlation times of their α carbons not longer than 20 ps could particularly contribute to the IINS spectrum of hydrated parvalbumin due to the substantial number of hydrogen atoms associated with the 19 Ala residues in pike 5.0 parvalbumin.

Isoleucyl residues

The isoleucyl side chains deserve special attention with regard to their dynamical properties. The Ile residues of parvalbumin are highly conserved during evolution (Kawasaki and Kretsinger, 1994). Three totally conserved Ile residues, at positions 50, 58, and 97 in the amino acid sequences, have their side chains forming a buried cluster within the hydrophobic core (see Fig. 9), as initially de-

scribed by Kretsinger and Nockolds (1973). The recent identification by x-ray crystallography at low temperature (100 K) with $PaCa_2$ crystals diffracting at 0.91 Å resolution (Declercq et al., 1999; submitted for publication) of several conformational substates of parvalbumin with positional variations in the angstrom range (involving residues such as Phe, Val, and Ile having internal side chains) indicates that parvalbumin corresponds to a highly integrated dynamical assembly with localized, as well as possibly concerted, motions. Due to the tight packing of the hydrophobic core it is likely that the different conformational substates, visualized as different molecular species at low temperature, possess some degree of overlapping, so that at higher temperature, under physiological conditions, these substates are interconverting in a concerted manner. Whatever the exact mechanisms of these conformational interconversions in space and time, the observation that both internal isoleucyl residues, Ile-58 and Ile-97, among other internally located residues, can be characterized by distinct substates suggests that some wobble exists within the hydrophobic core of parvalbumin. It is certainly not fortuitous that motions in the nanosecond time scale (see Results) were specifically detected in this work by NMR for the isoleucyl side chains. The fact that these motions appear at $h > 0.2$ (see Fig. 6) demonstrates that hydration is associated with the dynamics of the whole protein and not only with the structural elements which interact primarily with water molecules (polar and charged groups).

Sharpening the ^{13}C resonances upon hydration

There is still an open question concerning the origin of the narrowing of specific ^{13}C resonances in the solid-state ^{13}C-NMR spectra of powdered proteins at increasing hydration, as in the case of lysozyme (Kennedy and Bryant, 1990; Gregory et al., 1993a), bovine serum albumin (Gregory et al., 1993b) and parvalbumin (this work). The enhancement in spectral resolution with hydration has been attributed to a decrease in the distribution of isotropic chemical shifts as a consequence of a decrease in the distribution of conformational states sampled by the protein, rather than to rapid, large amplitude motional averaging of specific structural elements (Kennedy and Bryant, 1990; Gregory et al., 1993a). Such an interpretation is based on the fact that efficient dipolar coupling is preserved in the hydrated states, indicating that the conformational rearrangements that occur on hydration are small and do not involve any significant overall expansion of free volume or weakening of interactions that would increase the reorientational freedom of protein groups. This interpretation is in contrast with the aforementioned theoretical predictions (Steinbach and Brooks, 1993). At this point of our discussion it is interesting to mention a CP-MAS ^{13}C-NMR study of the hydration effects on the lineshapes of the ^{13}C resonances in a regular polypeptide, poly(L-lysine), which shows that the lysyl side-chain resonances respond in a systematic way to hydration with increased motion both as a function of increasing water content and as a function of distance from the main chain (Swanson and Bryant, 1991). There is indeed a net reduction in the linewidth of all lysyl side-chain ^{13}C resonances in poly(L-lysine) by a factor of ~3–4 when going from the dry to more hydrated states ($h > 0$, 16). The regularity of the polypeptide sequence precludes the occurrence of a large distribution of isotropic chemical shifts at low hydration even if the conformation, in the absence of hydration water, favors intramolecular contacts between the lysyl side chains and the main chain atoms. The resemblance between the selective narrowing of the lysyl $^{13}C_\epsilon$ and $^{13}C_\delta$ resonances in the solid-state ^{13}C-NMR spectra of parvalbumin and the narrowing of the same carbon resonances in poly(L-lysine), at increasing hydration, suggests that in both cases these specific effects involve an increase in the mobility of the lysyl side chain as a whole. A solid-state ^{13}C-NMR study of crystalline (fully hydrated) lysozyme showed that the lysyl $^{13}C_\epsilon$ resonances in the 41 ppm region of the spectrum display a relatively short longitudinal relaxation time of 0.4 s (mean value), indicating rapid tumbling in the 10 ns time range (Tuzi et al., 1992). Similarly, the T_1 values of the $^{13}C_\epsilon$ resonances of hydrated poly(L-lysine) powders (h up to 0.5) are in the 0.2–0.4 s range (at $h = 0.5$, $T_1 = 0.36$ s), indicating motions of the lysyl polar heads in the 10 ns. We note, however, that the situation of a hydrated lysyl polar head in lysozyme crystals differs from that encountered with partially hydrated protein powders. In the former, the Lys polar head is in contact with bulk-like water, while in the latter the hydrated polar head is only in contact with a few hydration water molecules (see Fig. 8 *C*).

To know the real incidence of progressive hydration on the dynamics of the lysyl side chains in powdered proteins in a more quantitative level will require a systematic study of the relaxation parameters (linewidth effects, T_1 values) at different observation frequencies (dispersion effects). This situation is not presently available with the systems reported so far using possibly ^{13}C-enriched lysyl residues.

Model of protein hydration

A model is proposed in Fig. 8 for summarizing the effects observed upon hydration at the level of different dynamical loci of the protein. In the dry state (Fig. 8 *A*), the protein is dynamically constrained with regard to its slow motions. In a low dielectric constant environment, the electrostatic contacts will be favored so that a peripheral lysyl side chain will be bent toward the protein surface, thus contributing to the general stiffness of the protein through strong intramolecular contacts. In contrast, in the presence of hydration water, these intramolecular contacts will be lost and replaced by water-protein contacts, as illustrated in Fig. 8 *B*. A lysyl side chain with its preferentially hydrated ammonium group will thus point toward the exterior of the protein with the consequence that the side chain becomes more and more mobile going from the α carbon to the ϵ carbon. This view is in agreement with theoretical predictions by molecular dynam-

ics (MD): 1) as discussed by Smith (1991), MD simulations with proteins in vacuo show a strong tendency for the peripheral side chains (usually hydrated based on crystallographic evidence) to be bent toward the protein surface in the absence of hydration water (see Fig. 8 *A*), thus altering the radius of gyration of the protein; 2) a similar conclusion was reached by Ahlström et al. (1987) in the case of parvalbumin by comparing their MD simulations in vacuo and in the presence of explicit water molecules. The parvalbumin molecule was predicted to be more contracted in vacuo than in the crystal structure; 3) also, Steinbach and Brooks (1993), using MD simulations with carboxymyoglobin at different hydration levels, observed a general increase of the radius of gyration of the protein at increasing hydration values. Interestingly, in the context of this work, these authors observed that the expansion of the protein involves not only the peripheral side chains but also the globular domain of the protein (see above).

In Fig. 8 *C* we include a view of a typical lysyl side chain, i.e., the external Lys-91 in the crystal structure of the isoform pI 4.10 from pike (1PVB; Declercq et al., 1996) which has been determined at atomic resolution (0.91 Å) and at low temperature (100 K) as recently reported (Declercq et al., 1999; submitted for publication). Lys-91 adopts to well-defined substates A and B at this low temperature. Lys-91 is also conserved in pike 5.0 parvalbumin. Each substate displays its own network of hydration water molecules with each ammonium polar head having three hydrogen-bonded water molecules, in agreement with the occurrence of a positively charged ammonium group with three hydrogen atoms. At ambient temperature, both lysyl substates are likely to be part of a dynamical exchange process. Butane-like molecules have torsional barriers up to 6 kcal/mol (Orville-Thomas, 1974), thus yielding reorientation constants in the range 10^7-10^8 s^{-1} (see Eq. 2 in Gelin and Karplus, 1975). Such reorientation constants could explain the changes in the half-widths of the ^{13}C resonances observed in the solid-state NMR spectra of $PaCa_2$ upon selective hydration of the peripheral lysyl side chains. Similarly, more rapid libration modes around the different single bonds of the lysyl side chains could contribute to the diffusion of hydrogen atoms within a confined volume, in the picosecond time scale, as observed by IQNS.

As stated above, the narrowing of the Ala $^{13}C_\beta$ and Ile $^{13}C_\delta$ resonances in the CP-MAS ^{13}C-NMR is interpreted as an increase in local mobility. The 19 Ala residues represent as many as 57 nonexchangeable hydrogen atoms (methyl groups), which could contribute to the diffusive motions observed by IQNS. The population of Ile residues could also contribute to IQNS with its 45 side-chain hydrogen atoms. Taken together, the side chains of Lys, Ala, and Ile, which are characterized by a selective narrowing of their side-chain ^{13}C resonances upon hydration as well as some of the side chains from Asp and Glu, could be part of the population of mobile protons ($1 - p = 30\%$, for a definition see Results) contributing through their motional properties to the observed IQNS variations. We conclude that the progressive hydration of parvalbumin is characterized by an increase in the local mobility of selected populations of hydrogen atoms until confined diffusive motions (with a mean diffusion coefficient of $0.68 \cdot 10^{-5}$ cm^2 s^{-1} within a spherical domain of radius 1.7 Å) are observed at $h = 0.65$ (see Fig. 5 *C*). At $h = 0.44$, the linewidth observed with $PaCa_2HDd$ (for a definition, see Materials and Methods) is closely related to the value expected on the plot Γ versus h established with a series of $PaCa_2HHd$ samples with $h = 0$, 0.12, 0.31, and 0.65 (not shown; Zanotti, 1997). The exchangeable hydrogen atoms therefore do not contribute significantly to the IQNS signal. Finally, Fig. 9 summarizes the situation by providing the positioning in the tertiary structure of $PaCa_2$ of two classes of side chains from Lys (*yellow*) and Ile (*red*), for which a marked dependence of their local dynamics on hydration is clearly inferred from our combined study of $PaCa_2$ by neutron scattering and NMR.

Functional significance of internal motions in parvalbumin

In Table 1 we summarize the types of motions detected so far in parvalbumin with the goal of comparing what is found with $PaCa_2$ in solution and with $PaCa_2$ in the hydrated powders and in the crystals. It is clear that the motions detected in the hydrated powders are closely related to the solution and crystal states. Due to the progressive variations of water activity upon hydration of a powdered protein, the studies with proteins in the solid state are fully relevant to our knowledge of the effects of hydration on protein structure and dynamics, as well as on protein function. It is not presently clear how the function of parvalbumin, as defined by its capacity to mediate Ca^{2+}/Mg^{2+} exchange under physiological conditions (Hou et al., 1992), is linked to internal dynamics. Our present work, which combines two physicochemical approaches with different time resolutions, is an attempt to meet this goal. It needs now to be established whether, and how, the motions detected by neutron scattering and by solid-state ^{13}C-NMR in the picosecond-nanosecond time scales are integrated in functionally relevant motions that could involve conformational substates for which lifetimes in the microsecond-millisecond range (or above) are expected to occur at physiological temperatures. Such a possible coupling between internal dynamics and protein function rests on the observation that the kinetic dissociation rates, or off-rate constants, in the range of 500 s^{-1} have been inferred for Ca^{2+} at physiological temperature (White, 1988). As part of the superfamily of the EF-hand proteins (Kawasaki and Kretsinger, 1994), parvalbumins appear closely related to physiological processes that involve cell excitation and relaxation, as in muscle and neurons (Rüegg, 1989; Berchtold et al., 1985; Celio, 1986). In the resting eukaryotic cell at low intracellular Ca^{2+} concentration, these EF-hand proteins are expected to be filled with Mg^{2+}, since the intracellular Mg^{2+} concentra-

TABLE 1 Summary of the different types of motions detected in parvalbumin $PaCa_2$ with their characteristic time-scales and amplitudes

Type of motion	Class of residue structural elements	Time scale (amplitude)	Biophysical method: data reduction	Ref.
Flipping motion about C_β-C_1 bonds	Phe (sc) (+ Tyr) $PaCa_2$/solution	$\mu s < t <$ ms ($\Delta\chi_2 \pm 180°$)	Liquid 1D ^{1}H-NMR: lineshape analysis	1
χ_1 Librations + coupling with mc dynamics	Phe (sc + mc) $PaCa_2$/solution	$\approx$ 4 ns (small $\Delta\chi_1$)	Liquid 1D ^{13}C-NMR: relaxation (anisotropic correlation times)	2
Fluctuations of ^{13}C-^{1}H vectors	Lys (sc) Ala (sc + mc) Ile (sc) $PaCa_2$/hydrated powder (h = 0.4)	~10 ns (undefined)	Solid-state ^{13}C-NMR: linewidths (isotropic correlation times)	This work
Fluctuations of ^{13}C-^{1}H vectors	all α-carbons (mc) $PaCa_2$/solution	1–60 ps (undefined)	Liquid 2D ^{1}H/^{13}C-NMR: relaxation (model free correlation times)	3
Confined diffusive motions of ^{1}H nuclei	Subpopulation of ^{1}H nuclei (from Lys, Ala, Ile, Asp, Glu) $PaCa_2$/hydrated powder (h = 0.65)	1–20 ps (<2 Å) $D = 0.68 \cdot 10^{-5}$ cm$^2 \cdot$ s^{-1}	IQNS	This work
Taxonomic substates	Phe-30* (sc + mc) $PaCa_2$/crystal hydrated	Undefined (1–2 Å)	X-ray crystallography atomic resolution (0.91 Å) low temperature (100 K)	4

Time scales are defined as lifetimes of a given substate (energy barrier-dependent interconversions between taxonomic substates), and by correlation times (distributions of statistical substates). D is a diffusion coefficient (diffusive motion in a confined domain). The amplitudes of motions are also given when known, in distance or angular units. Abbreviations used: mc, main chain; sc, side chain; h defines the hydration of the protein powder in grams of water/g dry protein (see text); $PaCa_2$ = fully calcium-loaded parvalbumin with two Ca^{2+} ions occupying both EF-hand cation-binding sites; taxonomic and statistical substates are used according to the terminology of Frauenfelder (1995a). References: 1, Cavé et al., 1976; 2, Nelson et al., 1976; 3, Alattia et al. (1996); 4, Declercq et al. (submitted for publication).
*Phe-30 is invariant during evolution.

tion is kept rather constantly in the millimolar range (Robertson et al., 1981; Hou et al., 1992). Upon muscle relaxation, as reviewed by Rüegg (1989), parvalbumin may take up the Ca^{2+} ions bound to troponin C (TnC) and calmodulin (CaM), among other calciproteins, because of its high affinity for Ca^{2+}, while Ca^{2+} may first bind to TnC and CaM because of low off-rates of Mg^{2+} from parvalbumin (Breen et al., 1985; White, 1988; Falke et al., 1994). As shown by Hou et al. (1992), using isolated frog skeletal muscle fibers, Pa facilitates muscle relaxation in the 0–20°C range due to a subtle balance between the temperature-dependence of the Ca^{2+} and Mg^{2+} dissociation rates from Pa and that of the Ca^{2+} uptake rate by the sarcoplasmic reticulum. Pa is present in relatively large amounts in the muscles of lower vertebrates, whereas in the higher vertebrates it is only present in relatively small amounts. The presence, however, of Pa in the central nervous system of higher vertebrates (Berchtold et al., 1985; Celio, 1986; Pfyffer et al., 1987; Blümcke et al., 1990; Hartig et al., 1996) raises the question of a more general role of Pa in the control of cell excitation and relaxation. Based on the order of magnitude of the off-rate constants for Ca^{2+} and Mg^{2+}, a correlation between slow dynamics (in the microsecond-millisecond range) within the parvalbumin core and the kinetics of cation dissociation appears as an attractive possibility thus intimately linking dynamics and function in this typical EF-hand protein.

Until now, several types of motions in parvalbumin are known as defined by their amplitudes and/or their frequencies, including our present results, as summarized in Table 1. However, they still represent a rather incomplete set in order to define the energy landscape of parvalbumin. Are all these motions reported in Table 1 converging toward parvalbumin function? As pointed out by Frauenfelder (1995a), one of the challenges in understanding the structure and dynamics of proteins is to establish a connection between the conformational substates (termed taxonomic substates) and protein function. Although the physiological role of parvalbumin is still undefined, at least in a detailed manner, the capacity of this typical EF-hand protein to bind Ca^{2+} and Mg^{2+} with different dissociation constants so that the k_{Ca}/k_{Mg} ratio of 10^{-3}-10^{-4} (Kawasaki and Kretsinger, 1994) has an intermediate value between the ratios of the intracellular ionic concentrations $[Ca^{2+}]_{int}/[Mg^{2+}]_{int}$ of 10^{-4}, at relaxation, and of 10^{-2}, at the onset of excitation, in excitable cells depending on Ca^{2+}-signaling, opens the possibility that the invariant k_{Ca}/k_{Mg} ratio of 10^{-3}-10^{-4} during vertebrate evolution is under the central of the internal dynamics of the protein. These thermodynamic features, as well as the kinetic features associated with Ca^{2+} and Mg^{2+} uptake and release (see above) are likely to be crucial under physiological conditions (Hou et al., 1992). At the structural level an important feature related to the capacity of parvalbumin to alternate between the Ca- and Mg-loaded forms was provided by the first determination of a crystal structure of parvalbumin with one of the EF-hands loaded with Mg^{2+} (Declercq et al., 1991). It was thus observed that the side chain of the invariant Glu-101 in the C-terminal EF hand site, EF-4 (or EF site) which ensures the coordination of the central cation along the z axis, undergoes a χ_1 transconformation, from g(+) to g(−), when substituting Ca^{2+} by Mg^{2+}. Glu-101 occupies the relative position 12 in the EF-hand loop. Due to the invariance of Glu in all parvalbumin EF-hands, this specific glutamyl residue is desig-

nated "Glu-12" here. Such an energy barrier-controlled interconversion of the "Glu-12" side chain that allows the protein to switch between two functional states (Ca^{2+}- and Mg^{2+}-loaded, respectively), suggests that the mobility of the hydrophobic core is crucial to the function of the protein, as initially hypothesized (Cavé and Parello, 1981). As stated above, a study by x-ray crystallography of $PaCa_2$ at atomic resolution (0.91 Å) and at low temperature (100 K), below the glassy transition of the protein (see Note 5), shows that several hydrophobic residues in the protein core adopt different conformational substates (Declercq et al., submitted for publication; see above). This is the case of the invariant Phe-30, as indicated in Table 1. This suggests that despite the dense organization of the hydrophobic core there is still the possibility for some wobbling inside this central unit, which hosts the different Phe χ_1 rotameric interconversions in the millisecond time scale, as initially reported (Cavé et al., 1976). There is evidence that the flipping energy barriers of specific Phe residues in parvalbumin are dependent on the nature of the cations bound to the protein, Ca^{2+} and Mg^{2+}, respectively (see ref. Parello et al., 1991 in Blancuzzi et al., 1993 and unpublished results by Cavé and Parello; see also Blancuzzi, 1993). Similarly, the analysis of the mean-square displacements of the ^1H nuclei by IINS shows that both forms are characterized by different displacements (Zanotti, 1997; Zanotti et al., 1997).

Altogether, structure and dynamics appear intimately linked in parvalbumin as part of the functioning of the protein as a Ca^{2+}/Mg^{2+} exchange protein. The tertiary structure of parvalbumin is organized in a single domain with all the different regions of the amino acid sequence contributing to the hydrophobic core (Kretsinger and Nockolds, 1973). Even small displacements of structural elements when the protein alternates between its Ca- and Mg-loaded forms (see Discussion in Declercq et al., 1991) might be responsible for the large effects observed at the level of the energetics of the protein-cation interactions (k_{Ca}/k_{Mg} ratio of 10^{-3}-10^{-4}). As recently suggested by theoretical simulations (Allouche et al., 1999), the small atomic displacements (in the 0.5 Å range or less) observed at the level of the cation-binding sites between both forms of parvalbumin, Ca- and Mg-loaded, account for the differences of free energy between both forms. Whereas the slow dynamics processes known to occur in parvalbumin (Table 1) can be envisaged as "taxonomic" conformational substates (Frauenfelder, 1995a), in the sense that they can be characterized and described individually (this the case of the substates visualized by x-ray crystallography at 100 K; Declercq et al., 1999; submitted for publication), the motions reported in this work with hydrated parvalbumin in the picosecond-nanosecond range are likely to correspond to statistical conformational substates (Frauenfelder, 1995a) which display only minor differences in their properties so that they cannot be identified individually and must be described by distributions. A taxonomic substate can exist in a very large number (probably in the 10^4 range and above) of statistical substates (Nienhaus et al., 1997). The present status with parvalbumin with regard to internal dynamics (Table 1) shows that some of the substates responsible for the slow dynamics are associated with energy barriers. Knowing such barriers quantitatively, as well as their variations upon Ca^{2+}/Mg^{2+} exchange, is of paramount importance to our knowledge of the functional aspects of a typical EF-hand protein. The crucial role of hydration on the dynamical regime of parvalbumin in the picosecond-nanosecond time scales, as demonstrated in this work by a parallel analysis of hydrated $PaCa_2$ powders by IINS and solid-state ^{13}C NMR, provides a first integrated view of parvalbumin dynamics in a controlled water environment.

Finally, the question arises to know whether the motions observed in the picosecond-nanosecond range through our combined experimental approach (IQNS and NMR) translate an adaptive trend in relation to parvalbumin function or are without any significance to function, which would correspond to an unavoidable "white noise" in the protein. This a central question in structural biology in its attempts to correlate protein dynamics and function. If one refers to the concept of hierarchical energy landscape in proteins, as pioneered by Frauenfelder (for a recent presentation, see Nienhaus et al., 1997), the distinct tiers of the landscape differ by the multiplicity of their conformational substates as well as by the heights of the energy barriers between substates within a given tier. As shown by Gelin and Karplus (1975) in their initial calculations of "flexible geometry energy barriers" within a globular protein (BPTI), the potential energy profiles of the Phe flipping motions (see text above) are highly sensitive to van der Waals contacts so that it is only upon release of such contacts during the flipping motion that realistic barriers could be predicted in agreement with experiment (NMR).

Due to the complexity (defined by the high multiplicity of, and the connectivity between, substates) of the interatomic contacts in a condensed environment as observed in proteins, it is likely that the energy profiles for most dynamical events correspond to rugged landscapes with a large number of local minima. This will have as a corollary that different proteins possess different energy landscapes due to the details in their tertiary folds. Our initial question thus becomes: *Are internal dynamics preserved within a given phylogenetically homologous family of proteins that are characterized by a common biological function?* Such a question can be addressed by taking advantage of the repertoire of homologous protein molecules available to us in the different extant species, as reporters of evolutionary trends. Parvalbumins that are ubiquitous in vertebrates offer such a possibility, as initially recognized by Goodman and Pechère (1977). A first ^1H-NMR study of parvalbumins from different species showed that the Phe flipping motions that are part of the repertoire of the parvalbumin slow dynamics were conserved during evolution, although only lower limits of the flipping rates (1000 s^{-1} or more at ambient temperature) could be determined at that time under the experimental conditions used (Cavé and Parello, 1981). Such a comparison between different parvalbumins

would require to further address this question at a more quantitative level (activation energy barriers) by using the largest field strengths presently available to high-resolution NMR.

At this level, it is relevant to ask which of the internal motions (as presented in Table 1) are effectively coupled to the local dynamics of the cation-binding sites and hence could intervene in the kinetic features of cation capture and release by the protein. In this respect, it appears necessary to consider whether the hydrophobic core is dynamically coupled to the cation-binding sites in its whole or only partially. A first answer can be found in the fact that most of the residues in the hydrophobic core of parvalbumin are totally conserved during evolution. A parallel analysis of the conformational multistates in the hydrophobic core of different parvalbumins by cryocrystallography, as first achieved with the isoform pI 4.10 from pike muscle (Declercq et al., 1999; submitted for publication), could be one approach with regard to the occurrence and maintenance of such multistates during evolution. Several pieces of evidence converge toward a correlation between the picosecond-nanosecond dynamics (as inferred in this work from neutron scattering and solid-state NMR) and parvalbumin function: 1) our CP-MAS ^{13}C-NMR relaxation study (linewidth analysis) of powdered $PaCa_2$ at varying hydration levels shows that specific loci in the tertiary structure (Fig. 9) are involved in the nanosecond dynamics; importantly, these loci are not restricted to external hydratable elements (i.e., the ammonium headgroups of the lysyl residues) but also occur within the hydrophobic core (Ile residues) where no water molecules are present; 2) such loci involve residues with a relatively large number of hydrogen atoms (see text above) and therefore likely contribute to the diffusive motions in the picosecond time scale that are inferred from the IQNS data. Mechanistically, the invariant loci Ile-50 and Ile-97 in the hydrophobic core are directly linked to the EF-hand cation-binding loops, EF-3 and EF-4, respectively. The wobble observed at the level of these internal loci, which appears in the regime of slow (interconversions between taxonomic substates in the microsecond-millisecond time scale) and fast dynamics (interconversions between statistical substates in the picosecond-nanosecond time scales), could be coupled to the dynamics of the loops EF-3 (or CD site) and EF-4 (or EF site) themselves and hence to the kinetics of cation capture and release by the cation-binding sites of parvalbumin. It must be noted that the helix-loop-helix (HLH) motif making up the EF-hand is a structurally integrated motif and it is not possible to dissociate the dynamics of the central loop from the motions of the entire HLH motif. Furthermore, it is well established that the EF-hand proteins only display pairs of EF-hands and never an odd number of EF-hands, due to the fact that the tertiary fold involves a pair of EF-hands connected through a central hydrophobic domain (core) as well as through hydrogen bonding between both loops in an antiparallel β-stranded arrangement (Strynadka and James, 1989). Presently, the coupling between the dynamics of the hydrophobic core of parvalbumin and the capacity of the protein to alternate between the Ca- and Mg-loaded forms under physiological conditions remains a hypothesis, as initially proposed (Cavé and Parello, 1981).

As stated by Nienhaus et al. (1997), some, if not all, of the protein fluctuations will depend on the solvent surrounding the protein, so that protein and environment must be treated together. Our combined study of parvalbumin dynamics by IQNS and NMR explores a range of hydration from $h = 0$ ("dry" protein) to $h = 0.65$. The latter h value goes beyond hydration of the complete surface by a water monolayer ($\sim$300 water molecules, i.e., $h = \sim 0.45$ g/g, would be necessary to cover the surface of the protein calculated according to Miller et al., 1987) so that our dynamical measurements with the hydrated $PaCa_2$ powders were carried out under conditions comparable to those found in parvalbumin crystals. Another open question deals with the real state of the hydration of proteins (and biomacromolecules in general) in the highly compartmentalized interior of a cell, which fundamentally departs from the conditions used in vitro with "dilute" solutions.

Taken together, all these pieces of information suggest that the internal dynamics of parvalbumin are correlated to the nature of the cation bound in the EF-3 and EF-4 sites. It might be that an essential piece of the puzzle is the coupling between the dynamics of the topologically invariant hydrophobic core and the dynamics of the cation-binding sites. We tentatively conclude that the reduction in internal mobility of $PaMg_2$ relative to $PaCa_2$ (Zanotti, 1997; to be published) is directly responsible for the differences in the kinetics rate of cation dissociation, k_{off}, between both cations, Mg^{2+} and Ca^{2+}.

Upon muscle relaxation, as reviewed by Rüegg (1989), parvalbumin may take up the Ca^{2+} ions bound to TnC and CaM, among other calciproteins, because of its high affinity for Ca^{2+}, while Ca^{2+} may bind first to TnC and CaM because of a slow off-rate of Mg^{2+} from parvalbumin (Breen et al., 1985; White, 1988; Falke et al., 1994). The maintenance of distinct dissociation rates for Ca^{2+} and Mg^{2+} in parvalbumin is likely to be at the heart of the biological function of this "ancillary" calciprotein (Rüegg, 1989). In closing, it is our belief that a comprehensive description of parvalbumin dynamics will help understand the physiological role of parvalbumin and its specificity among other calciproteins that are involved in cell excitation and relaxation.

CONCLUSIONS

We have observed that hydration has a major influence on the dynamics of a globular protein such as parvalbumin. The motions detected by two experimental approaches, IQNS and solid-state ^{13}C-NMR, differ markedly in their time scales, with correlation times in the 10–20 ps range (short time diffusive motions) and in the 10 ns range, respectively. Both experimental approaches indicate an increase in the

protein dynamics upon progressive hydration of the dry protein. It is not only the polar side chains at the surface of the protein that are primarily affected during the early steps of hydration, as expected, but also internal nonpolar side chains. These results suggest that hydration acts on the dynamics of the protein at both local and global levels. Although restricted to a relatively narrow time range (picosecond-nanosecond), our combined study by IQNS and NMR allows, for the first time, identification of specific sites or loci in the tertiary structure that are involved in the dynamics of parvalbumin, as is the case of the external lysyl residues but also the alanyl residues occupying an intermediate position between the surface and the interior, as well as the internal isoleucyl residues. Our present observations will thus help map the energy landscape of the protein if combined with theoretical predictions. It is known that other loci in the tertiary structure of parvalbumin are part of the dynamical repertoire of the protein. The observation of different substates at the level of several loci within the hydrophobic core of parvalbumin by cryocrystallography ("frozen" substates) indicates that this internal domain is a dynamical assembly that hosts a large spectrum of events encompassing rapid ($< \mu$s) and slow ($> \mu$s) dynamics. Such loci could thus correspond to wobbly spots in the tertiary structure and host well-defined taxonomic substates as part of the higher tiers of the protein energy landscape. The fact that the internal isoleucyl residues undergo a selective variation in their motional regime in the picosecond-nanosecond time scale upon hydration of powdered $PaCa_2$, as inferred in this work from IQNS and NMR, appears in line with the results of the aforementioned cryocrystallographic study. Such wobbly spots might finally be related to the function of the protein. Motions in the lower tiers (rapid dynamics in the picosecond-nanosecond range) of the protein energy landscape could be related to, and possibly control, motions in the higher tiers of the landscape (in the microsecond-millisecond range). The rapid dynamics of parvalbumin in the picosecond-nanosecond time scales likely contribute to the ruggedness of the potential profiles, but if such local energy barriers are, as expected, in the order of kT at ambient temperature, they will be perceived as diffusive motions by IQNS and as Brownian-type motions in ^{13}C-NMR relaxation. Our observation by IQNS and NMR with hydrated $PaCa_2$ (at $h > 0.4$ g water/g dry protein) that the diffusive motions of hydrogen atoms in the 10–20 ps range are restricted within a confined volume (sphere not exceeding 2 Å in radius) agrees well with the consensus that proteins correspond to condensed systems with constrained dynamics. The apparently high mobility of the hydrophobic core of parvalbumin encompassing multiple dynamical events in the picosecond-nanosecond time scales (this work) up to milliseconds (Phe flipping motions, as inferred from previous lineshape NMR studies) could thus be related in a hierarchical manner to the function of parvalbumin in Ca^{2+}-excitable cells by controlling the capture and release of both divalent cations, Ca^{2+} and Mg^{2+}. This appears as a very attractive possibility, which will require a more extended investigation, at both experimental and theoretical levels, of both forms of parvalbumin, Ca^{2+}- and Mg^{2+}-loaded. Finally, we present a rather complete survey of our present knowledge of parvalbumin dynamics thus indicating where gaps are already filled and where more experiments are needed.

NOTES

1. The density of coherent scattering length of a medium composed of N atoms of coherent scattering length b_i is defined as $\rho = \Sigma^N b_i/V$, where V is the specific volume of the medium.

2. The chemical shifts in Nelson et al. (1976) are reported with respect to an external tetramethylsilane reference so that chemical shift values adopted in our work with respect to the internal reference TSP-d4 (see Materials and Methods; Alattia et al., 1996) could differ from theirs. Nelson et al. (1976) reported the lysyl $^{13}C_\epsilon$ resonances at ~39 ppm instead of 41.9 ppm in Alattia et al. (1996).

3. We note that the crystal forms of parvalbumin with V_M values (i.e., the crystal volume per unit of protein molecular weight, as initially defined by Matthews, 1968) as low as 1.93 $Å^3 \cdot Da^{-1}$ (Declercq et al., submitted for publication) corresponds to a hydration value of $h = \sim 0.4-0.5$ g water/g protein (or less, if the precipitant molecules of ammonium sulfate are taken into account). It therefore appears that hydration in parvalbumin crystals and in protein crystals in general (a mean V_M value of 2.6 $Å^3 \cdot Da^{-1}$ was reported by Matthews (1968) based on a collection of 116 crystalline proteins) is related to the upper h values used here in our study of hydration-coupled dynamics with powdered $PaCa_2$ samples.

4. This number includes the protonated ammonium, imidazolium, and guanidinium groups from Lys, His, and Arg, respectively, and exclusively carboxylates from Asp and Glu.

5. An IINS study of both $PaCa_2$ and $PaMg_2$ forms (powdered samples at $h = \sim 0.2$) as a function of temperature (10–350 K) showed that the intensity of the elastic component behaves in a similar manner (Parello, unpublished results with IN13 spectrometer, ILL, Grenoble, France) to that previously observed with myoglobin (Doster et al., 1989) and other proteins.

We thank Drs. G. Etienne (CNRS, Montpellier, France) for assistance in the preparation of the parvalbumin samples, M. Ribet (University of Montpellier) for guidance during the NMR experiments, and R. Kahn for help during the neutron scattering experiments. We are also indebted to the reviewers for fruitful suggestions.

The authors are indebted to the Centre National de la Recherche Scientifique and Commissariat à l'Energie Atomique (France) for financial support. Prof. J. Durup is acknowledged for a fruitful discussion and for financial support (CNRS Grant GDR l150).

REFERENCES

Ahlström, P., O. Teleman, B. Jönsson, and S. Forsén. 1987. Molecular dynamics simulation of parvalbumin in aqueous solution. *J. Am. Chem. Soc.* 109:1541–1551.

Alattia, T., A. Padilla, and A. Cavé. 1996. Assignment of ^{13}C resonances and analysis of relaxation properties and internal dynamics of pike parvalbumin by ^{13}C-NMR at natural abundance. *Eur. J. Biochem.* 237: 561–574.

Allanche, D., J. Parello, and Y.-H. Sanejouand 1999. Ca^{2+}/Mg^{2+} exchange in parvalbumin and other EF-hand proteins: a theoretical study. *J. Mol. Biol.* 285:857–873.

Andreani, C., A. Filabozzi, F. Menzinger, A. Desideri, A. Deriu, and D. Di Cola. 1995. Dynamics of hydrogen atoms in superoxide dismutase by quasi-elastic neutron scattering. *Biophys. J.* 68:2519–2523.

Ansari, A., J. Berendzen, S. F. Bowne, H. Frauenfelder, I. E. Iben, T. B. Sauke, E. Shyamsunder, and R. D. Young. 1985. Protein states and proteinquakes. *Proc. Natl. Acad. Sci. USA*. 82:5000–5004.

Baldellon, C., A. Padilla, and A. Cavé. 1992. Kinetics of amide proton exchange in parvalbumin studied by ^{1}H 2D-NMR. A comparison of the calcium and magnesium loaded forms. *Biochimie*. 74:837–844.

Bauer, D. R., S. J. Opella, D. J. Nelson, and R. Pecora. 1974. Depolarized light scattering and carbon nuclear resonance measurements of the isotropic rotational correlation time of muscle calcium binding protein. *J. Am. Chem. Soc.* 97:2580–2582.

Bée, M. 1988. Quasielastic Neutron Scattering: Principles and Applications in Solid-State Chemistry, Biology and Material Science. Adam and Hilger, Bristol and Philadelphia.

Bellissent-Funel, M.-C., J. Lal., K. F. Bradley, and S. H. Chen. 1993. Neutron structure factors of in vivo deuterated amorphous protein C-phycocyanin. *Biophys. J.* 64:1542–1549.

Bellissent-Funel, M.-C., J.-M. Zanotti, and S. H. Chen. 1996. Slow dynamics of water molecules on the surface of a globular protein. *Faraday Discuss.* 103:281–294.

Berchtold, M. W., M. R. Celio, and C. W. Heizmann. 1985. Parvalbumin in human brain. *J. Neurochem.* 45:235–240.

Blancuzzi, Y. 1993. Etude par RMN protonique de l'échange Ca^{2+}/Mg^{2+} en série calciprotéine (parvalbumine de brochet, pI 5,0). PhD Thesis. University of Montpellier II. 54–56.

Blancuzzi, Y., A. Padilla, J. Parello, and A. Cavé. 1993. Symmetrical rearrangement of the cation-binding sites of parvalbumin upon Ca^{2+}/Mg^{2+} exchange. A study by 1H 2D NMR. *Biochemistry.* 32:1302–1309.

Blümcke, I., P. R. Hof, J. H. Morrison, and M. R. Celio. 1990. Distribution of parvalbumin in the visual cortex of old monkeys and humans. *J. Comp. Neurol.* 301:417–432.

Breen, P. J., K. A. Johnson, and W. D. Horrocks. 1985. Stopped-flow kinetic studies of metal ion dissociation or exchange in a tryptophan-containing parvalbumin. *Biochemistry.* 24:4997–5004.

Bryant, R. G. 1996. The dynamics of water protein interactions. *Annu. Rev. Biophys. Biomol. Struct.* 25:29–53.

Cavé, A., M. F. Daurès, J. Parello, A. Saint-Yves, and R. Sempéré. 1979b. NMR studies of primary and secondary sites of parvalbumins using the two paramagnetic probes Gd(III) and Mn(II). *Biochimie.* 61:755–765.

Cavé, A., C. M. Dobson, J. Parello, and R. J. P. Williams. 1976. Conformational mobility within the structure of muscular parvalbumins. An NMR study of the aromatic resonances of phenylalanine residues. *FEBS Lett.* 65:190–194.

Cavé, A., M. Pagès, P. Morin, and C. Dobson. 1979a. Conformational studies on muscular parvalbumins cooperative binding of calcium(II) to parvalbumins. *Biochimie*. 61:607–613.

Cavé, A., and J. Parello. 1981. Dynamic aspects of the structure of globular proteins by high-resolution nmr spectroscopy. The fluid-like structure of the internal hydrophobic core of muscular parvalbumins. *In* Les Houches, Session XXXIII, 1979: Membranes and Intercellular Communication. R. Balian, M. Chabre, and P. F. Devaux, editors. North-Holland Publishing Co., Amsterdam. 197–227.

Celio, M. R. 1986. Parvalbumin in most γ-aminobutyric acid-containing neurons of the rat cerebral cortex. *Science.* 213:995–997.

Cusack, S., and W. Doster. 1990. Temperature dependence of the low frequency dynamics of myoglobin. *Biophys. J.* 58:243–251.

Declercq, J. P., C. Evrard, D. C. Carter, B. S. Wright, G. Etienne, and J. Parello. 1999. A crystal of a typical EF hand protein grown under microgravity diffracts x-rays at a resolution beyond 0.9 Å. *J. Cryst. Growth.* 196:595–601.

Declercq, J. P., B. Tinant, and J. Parello. 1996. X-ray structure of a new crystal form of pike 4.10β parvalbumin. *Acta. Crystallogr., Sect. D.* 52:165–169.

Declercq, J. P., B. Tinant, J. Parello, and J. Rambaud. 1991. Ionic interactions with parvalbumins. Crystal structure determination of pike 4.10 parvalbumin in four different ionic environments. *J. Mol. Biol.* 220: 1017–1039.

Doster, W., S. Cusack, and W. Petry. 1989. Dynamical transition of myoglobin revealed by inelastic neutron scattering. *Nature.* 337: 754–756.

Drexel, W., and W. L. Peticolas. 1975. Neutron-scattering spectroscopy of the α- and β-forms of poly-L-alanine. Motion of the methyl side chain. *Biopolymers.* 14:715–721.

Falke, I. J., S. K. Drake, A. L. Hazard, and O. B. Persen. 1994. Molecular tuning of ion binding to calcium signaling proteins. *Q. Rev. Biophys.* 27:219–290.

Ferrand, M., A. J. Dianoux, W. Petry, and G. Zaccaï. 1993. Thermal motions and function of bacteriorhodopsin in purple membranes: effects of temperature and hydration studied by neutron scattering. *Proc. Natl. Acad. Sci. USA.* 90:9668–9672.

Fitter, J., R. E. Lechner, and N. A. Dencher. 1997. Picosecond molecular motions in bacteriorhodopsin from neutron scattering. *Biophys. J.* 73: 2126–2137.

Frauenfelder, H., and E. Gratton. 1986. Protein dynamics and hydration. *Methods Enzymol.* 127:207–216.

Frauenfelder, H. 1989. New looks at protein motions. *Nature.* 338: 623–624.

Frauenfelder, H. 1995a. Complexity in proteins. *Nat. Struct. Biol.* 2:821–823.

Frauenfelder, H. 1995b. Proteins-paradigms of complex systems. *Experientia.* 51:200–203.

Frauenfelder, H. 1998. Dynamics and function of proteins: the search for general concepts. *Proc. Natl. Acad. Sci. USA.* 95:4795–4796.

Frey, M. 1993. Water structure of crystallized proteins: high resolution studies. *In* Water and Biological Macromolecules. Topics in Molecular and Structural Biology. E. Westhof, editor. MacMillan, London. 17: 98–147.

Gavish, B., E. Gratton, and C. J. Hardy. 1983. Adiabatic compressibility of globular proteins. *Proc. Natl. Acad. Sci. USA.* 80:750–754.

Gelin, B. R., and M. Karplus. 1975. Sidechain torsional potentials and motions of amino acids in proteins: bovine pancreatic trypsin inhibitor. *Proc. Nat. Acad. Sci. USA*. 72:2002–2006.

Gerstein, M., A. M. Lesk, and C. Chotia. 1994. Structural mechanisms for domain movement in proteins. *Biochemistry.* 33:6739–6749.

Goodman, M., and J. F. Pechère. 1977. The evolution of muscular parvalbumins investigated by the maximum parsimony method. *J. Mol. Evol.* 9:131–158.

Gregory, R. B., M. Gangoda, R. K. Gilpin, and W. Su. 1993a. The influence of hydration on the conformation of lysozyme studied by solid-state ^{13}C-NMR spectroscopy. *Biopolymers*. 33:513–519.

Gregory, R. B., M. Gangoda, R. K. Gilpin, and W. Su. 1993b. The influence of hydration on the conformation of bovine serum albumin studied by solid-state NMR. *Biopolymers*. 33:1871–1876.

Gurd, F. R. N., and T. M. Rothgeb. 1979. Motions in proteins. *Adv. Protein Chem.* 33:73–165.

Halle, B., T. Andersson, S. Forsén, and B. Lindman. 1981. Protein hydration from water oxygen-17 magnetic relaxation. *J. Am. Chem. Soc.* 103:500–508.

Hartig, W., G. Bruckner, K. Brauer, G. Seeger, and V. Bigl. 1996. Triple immunofluorescence labelling of parvalbumin, calbindin-D28K and calretinin in rat and monkey brain. *J. Neurosci. Methods.* 67:89–95.

Henry, G. D., J. H. Weiner, and B. D. Sykes. 1986. Backbone dynamics of a model membrane protein: ^{13}C-NMR spectroscopy of alanine methyl groups in detergent-solubilized M13 coat protein. *Biochemistry.* 25: 590–598.

Hou, T. T., J. D. Johnson, and J. A. Rall. 1992. Effect of temperature on relaxation rate and Ca^{2+}, Mg^{2+} dissociation rates from parvalbumin of frog muscles. *J. Physiol.* 449:339–410.

Jacrot, B., S. Cusack, A. J. Dianoux, and D. M. Engelman. 1982. Inelastic neutron scattering analysis of hexokinase dynamics and its modification on binding of glucose. *Nature.* 300:84–86.

Jardetzky, O., and N. G. Wade-Jardetzky. 1980. Comparison of protein structures by high resolution solid state and solution NMR. *FEBS Lett.* 110:133–135.

Kawasaki, H., and R. H. Kretsinger. 1994. Calcium-binding proteins. 1: EF-hand proteins. *Protein Profile*. 1:343–517.

Kennedy, S. D., and R. G. Bryant. 1990. Structural effects of hydration: studies of lysozyme by ^{13}C Solids NMR. *Biopolymer.* 29:1801–1806.

Kneller, G. R., W. Doster, M. Settles, S. Cusack, and J. C. Smith. 1992. Methyl group dynamics in the crystalline alanine dipeptide: a combined

computer simulation and inelastic neutron scattering. *J. Chem. Phys.* 97:8864–8879.

Komoroski, R. A. 1986. High-Resolution NMR Spectroscopy of Synthetic Polymers in Bulk, Chaps. 2 and 4. R. A. Komoroski, editor. VCH Publishers, Deerfield Beach, FL.

Korzhnev, D. M., V. Y. Orekhov, and A. S. Arseniev. 1997. Model-free approach beyond the borders of its applicability. *J. Magn. Reson.* 127: 184–191.

Kretsinger, R. H., and C. E. Nockolds. 1973. Carp muscle calcium-binding protein. II. Structure determination and general description. *J. Biol. Chem.* 248:3313–3326.

Lovesey, S. W. 1987. Theory of Neutron Scattering from Condensed Matter, 3rd ed. Clarendon Press, Oxford.

Matthews, B. W. 1968. Solvent content of protein crystals. *J. Mol. Biol.* 33:491–497.

McCammon, J. A. 1984. Protein dynamics. *Rep. Prog. Phys.* 47:1–46.

Miller, S., J. Janin, A. M. Lesk, and C. Chotia. 1987. Interior and surface of monomeric proteins, *J. Mol. Biol.* 196:641–656.

Nelson, D. J., S. J. Opella, and O. Jardetzky. 1976. ^{13}C nuclear magnetic resonance study of molecular motions, and conformational transitions in muscle calcium binding parvalbumins. *Biochemistry.* 15:5552–5560.

Nienhaus, G. U., I. D. Müller, B. H. McMahon, and H. Frauenfelder. 1997. Exploring the conformational landscape of proteins. *Physica D.* 107: 297–311.

Opella, S. J. 1975. Carbon-13 nuclear magnetic resonance study of muscle calcium binding protein. Ph.D. thesis, Stanford University.

Opella, S. J. 1997. NMR and membrane proteins. *Nat. Struct. Biol.* 4(Suppl):845–848.

Opella, S. J., D. J. Nelson, and O. Jardetzky. 1974. Carbon magnetic resonance of the conformational changes in carp muscle calcium binding parvalbumin. *J. Am. Chem. Soc.* 96:7157–7159.

Orville-Thomas, W. J., editor. 1974. Internal Rotation of Molecules. John Wiley and Sons, London, New York. 1–18.

Otting, G., E. Liepinsh, and K. Wüthrich. 1991. Protein hydration in aqueous solution. *Science.* 254:974–980.

Padilla, A., A. Cavé, and J. Parello. 1988. Two-dimensional ^{1}H nuclear magnetic resonance study of pike pI 5.0 parvalbumin (*Esox lucius*). Sequential resonance assignments and folding of the polypeptide chain. *J. Mol. Biol.* 204:995–1017.

Parello, J., A. Cavé, S. Cusack, Y. Blancuzzi, and A. Padilla. 1991. European Research Conference 1991. Research Conference on NMR in Molecular Biology, Heemskerk, The Netherlands, May 20–24.

Parello, J., A. Cavé, P. Puigdomènech, C. Maury, J.-P. Capony, and J.-F. Pechère. 1974. Conformational studies on muscular parvalbumins. II. Nuclear magnetic resonance analysis. *Biochimie.* 56:61–76.

Parello, J., and J. F. Pechère. 1971. Conformational studies on muscular parvalbumins. I. Optical rotatory dispersion and circular dichroism analysis. *Biochimie.* 53:1079–1083.

Pechère, J.-F., J. Demaille, and J.-P. Capony. 1971. Muscular parvalbumins: preparative and analytical methods of general applicability. *Biochem. Biophys. Acta.* 236:391–408.

Perutz, M. F. 1946. The composition and swelling properties of haemoglobin crystals. *Trans. Faraday Soc.* 47B:187–197.

Pfyffer, G. E., A. Faivre-Bauman, A. Tixier-Vidal, A. W. Norman, and C. W. Heizmann. 1987. Developmental and functional studies of parvalbumin and calbindin D28k in hypothalamic neurons grown in serum-free medium. *J. Neurochem.* 49:442–451.

Qian, Y. Q., G. Otting, and K. Wüthrich. 1993. NMR detection of hydration water in the intermolecular interface of a protein-DNA complex. *J. Am. Chem. Soc.* 115:1189–1190.

Réat, V., H. Patzelt, M. Ferrand, C. Pfister, D. Oesterhelt, and G. Zaccaï. 1998. Dynamics of different functional parts of bacteriorhodopsin: H-^{2}H labeling and neutron scattering. *Proc. Natl. Acad. Sci. USA*. 95: 4970–4975.

Réat, V., G. Zaccai, M. Ferrand, and C. Pfister. 1997. Functional dynamics in purple membrane. *In* Biological Macromolecular Dynamics. S. Cusack, H. Buttner, M. Ferrand, P. Langan, and P. Timmins, editors. Adenine Press, New York. 117–122.

Richards, F. M. 1977. Areas, volume, packing and protein structure. *Annu. Rev. Biophys. Bioeng.* 6:151–176.

Robertson, S. P., J. D. Johnson, and J. D. Potter. 1981. The time-course of Ca^{2+} exchange with calmodulin, troponin, parvalbumin, and myosin in response to transient increases in Ca^{2+}. *Biophys. J.* 34:559–569.

Roquet, F., J.-P. Declercq, B. Tinant, J. Rambaud, and J. Parello. 1992. Crystal structure of the unique parvalbumin component from muscle of the leopard shark (*Triakis semifasciata*). The first x-ray study of an α-parvalbumin. *J. Mol. Biol.* 223:705–720.

Rossky, P. J., and M. Karplus. 1979. A molecular dynamics study of a dipeptide in water. *J. Am. Chem. Soc.* 101:1913–1936.

Rüegg, J. C.. 1989. Calcium in Muscle Activation. Springer-Verlag, Berlin.

Rupley, J. A., and G. Careri. 1991. Protein hydration and function. *Adv. Protein Chem.* 41:37–172.

Savage, H., and A. Wlodawer. 1986. Determination of water structure around biomolecules using x-ray and neutron diffraction methods. *Methods Enzymol.* 127:162–183.

Smith, J. C. 1991. Protein dynamics: comparison of simulations with inelastic neutron scattering experiments. *Q. Rev. Biophys.* 24:227–291.

Steinbach, P. J., and R. Brooks. 1993. Protein hydration elucidated by molecular dynamics simulation. *Proc. Natl. Acad. Sci. USA.* 90: 9135–9139.

Strynadka, N. C. J., and M. N. G. James. 1989. Crystal structure of the helix-loop-helix calcium binding proteins. *Annu. Rev. Biochem.* 58: 951–998.

Swanson, S. D., and R. G. Bryant. 1991. The hydration response of poly(L-lysine) dynamics measured by ^{13}C-NMR spectroscopy. *Biopolymers.* 31:967–973.

Teixeira, J. 1992. Introduction to small angle neutron scattering applied to colloidal science. *In* Structure and Dynamics of Strongly Interacting Colloids and Supramolecular Aggregates in Solution. S.-H. Chen, J. S. Huang, and P. Tartaglia, editors. Kluwer, London. 635–658.

Thanki, N., J. M. Thornton, and J. M. Goodfellow. 1988. Distribution of water around amino acid residues. *J. Mol. Biol.* 202:637–657.

Tuzi, S., K. Shinzawa-Itoh, T. Erata, A. Naito, S. Yoshikawa, and H. Saito. 1992. A high-resolution solid-state ^{13}C-NMR study on crystalline bovine heart cytochrome-c oxidase and lysozyme. Dynamic behavior of protein and detergent in the complex. *Eur. J. Biochem.* 208:713–720.

Volino, F., and A. J. Dianoux. 1980. Neutron incoherent scattering law for diffusion in a potential of spherical symmetry. *Mol. Phys.* 41:271–279.

Westhof, E., editor. 1993. Water and Biological Macromolecules. Topics in Molecular and Structural Biology, Vol. 17. MacMillan, London.

White, H.-D. 1988. Kinetic mechanism of calcium binding to whiting parvalbumin. *Biochemistry*. 27:3357–3365.

Wider, G. 1998. Technical aspects of NMR spectroscopy with biological macromolecules and studies of hydration in solution. *Prog. Nucl. Magn. Reson. Spectr.* 32:193–275.

Zanotti, J.-M. 1997. Structure et dynamique de l'eau interfaciale. Rôle de l'eau d'hydratation dans la dynamique des protéines globulaires. Thèse de l'Université Paris XI.

Zanotti, J.-M., M.-C. Bellissent-Funel, and J. Parello. 1997. Dynamics of a globular protein as studied by neutron scattering and solid-state NMR. *Physica B.* 234–236:228–230.